2022 迷你應用文集

第三期 - 強大且靈活的分析基因治療和寡核苷酸藥物

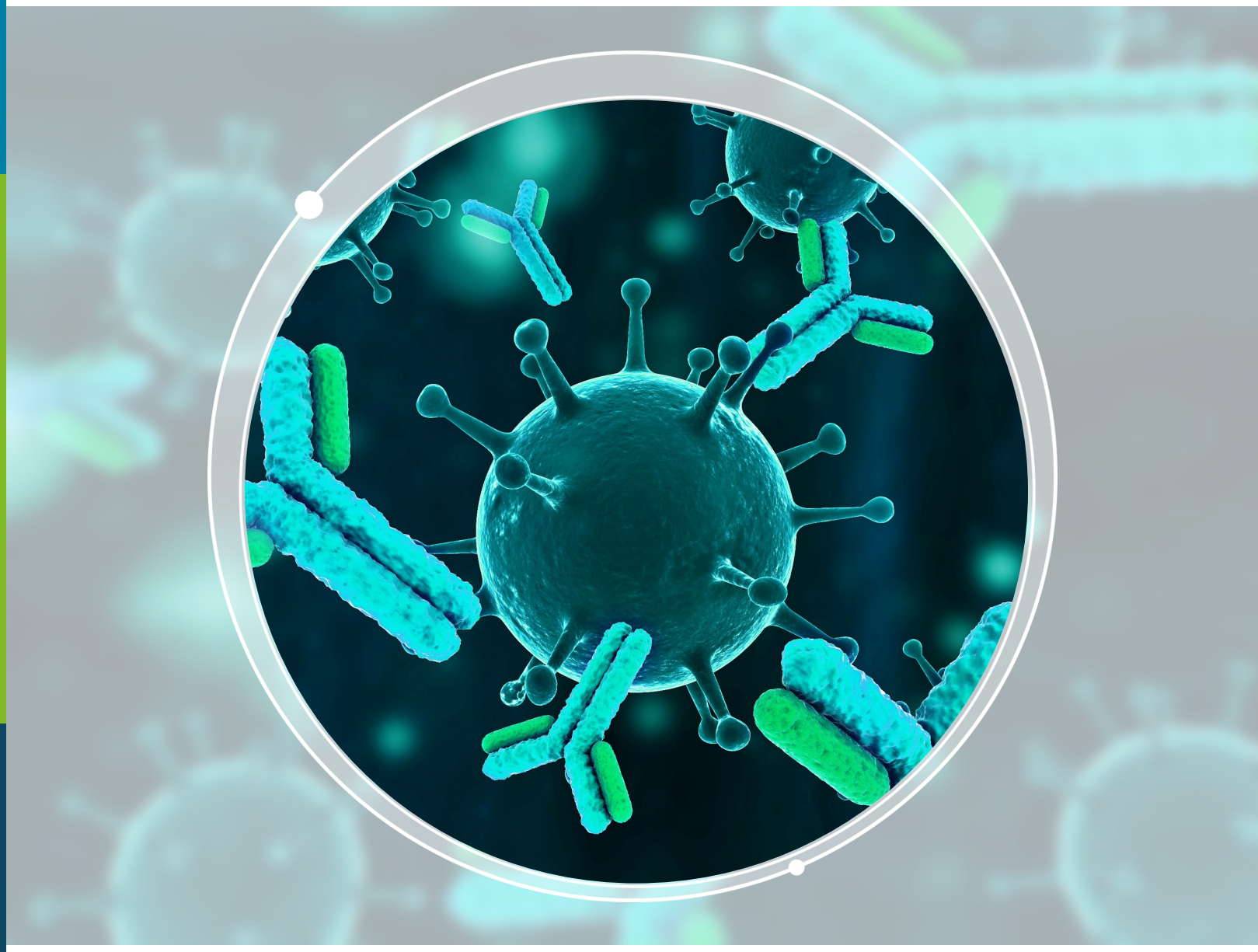

SCIEX

The Power of Precision

目錄

Analyzing the restriction fragments of gene therapy products by capillary electrophoresis with laser-induced fluorescence (CE-LIF) detection

Using the PA 800 Plus system

Ren Tingjun[1], Li Xiang[2] and Chen Hongxu[1]
[1]SCIEX, China; [2]National Institutes for Food and Drug Control

Introduction

With the rapid development of gene therapy-related research and technology in recent years, more and more gene therapy products will reach the market. Therefore, there is a growing need for suitable analytical methods for quality control of gene therapy products. Capillary electrophoresis (CE) is a separation technique that plays an essential role in biotechnology research, development and quality control. It is fully automated and environmentally friendly, while offering high resolution, good repeatability and high sensitivity with low reagent consumption requirements. This study employed the capillary electrophoresis PA 800 Plus system (Figure 1) to analyze the nucleic acid of a gene therapy product using herpes simplex virus (HSV) as the vector. The nucleic acid was cleaved into DNA fragments of differing lengths using restriction endonuclease (Nde I). By using a laser-induced fluorescence (LIF) detector, this study establishes a CE-LIF analysis method to identify the restriction profile of the gene therapy product vector. This study also demonstrates the robustness of the CE-LIF method and its comparability with agarose gel electrophoresis.

Figure 1. PA 800 Plus system.

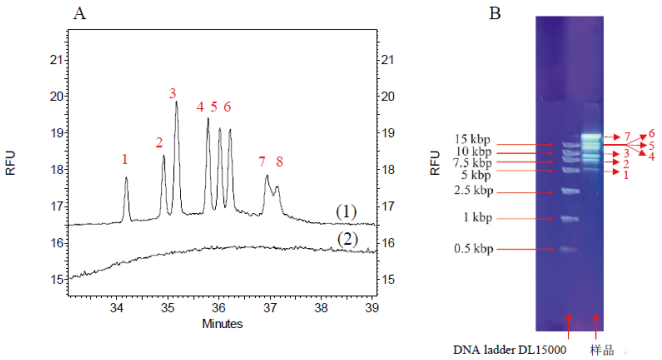

Figure 2. Analysis of restriction fragments in sample using CE-LIF or agarose gel electrophoresis methods. A: Analysis of restriction fragments in sample (1) using the CE-LIF method, compared to a blank control of DDI water (2). Conditions for CE-LIF: DNA-coated capillary with 50 µm inner diameter and 30 or 40 cm effective length, 3 s injection at 0.5 psi, -7 kV separation voltage, 40 min separation time, 4°C sample storage temperature, 25°C capillary temperature, 488 nm excitation wavelength and 520 nm detection wavelength. B: Analysis of restriction fragments in sample using the agarose gel electrophoresis method.

Gene therapy integrates modern biotechnology with clinical medicine and other disciplines. It defines a new approach for treating and studying major human diseases, such as malignant tumors, cardiovascular diseases, genetic diseases and autoimmune diseases. To monitor quality control for gene therapy products, identification tests are often performed at the nucleic acid and protein levels. At the nucleic acid level, appropriate restriction enzymes must be selected to produce restriction fragments that fully reflect the integrity of the nucleic acid in gene therapy products and that separate clearly during electrophoresis. This technical note demonstrates an application in which CE-LIF is used for restriction fragment analysis of gene therapy products.

Key Feature

- Simple steps for method optimization for the analysis of DNA fragments from a gene therapy vector

Methods

Sample Preparation: The sample was an HSV vector gene therapy product provided by the Recombinant Lab at the National Institutes for Food and Drug Control. The genomic material from the HSV vector was digested using Nde I endonuclease restriction enzyme.

Capillary Electrophoresis: The PA 800 Plus system (SCIEX, USA) running 32 Karat software 10.1, was equipped with a laser-induced fluorescence detector with excitation and emission wavelengths at 488 nm and 520 nm, respectively.

Reagents and consumables: The dsDNA 1000 kit (SCIEX, PN 477410) included the DNA-coated capillary, dsDNA 1000 Gel Buffer, dsDNA Test Mix and Orange G Reference Marker. Other reagents included SYBR Gold nucleic acid (Invitrogen, PN S11494), DL15000 DNA marker (Solarbio, PN M1700) and Tris Borate EDTA (10X TBE, PN Sigma T4323).

CE conditions: The DNA-coated capillary had a 50 µm inner diameter and 30 and 40 cm effective and total lengths, respectively. The injection and separation conditions used were 0.5 psi, 3 s and -7 kV for 40 min. The samples were stored at 4°C and the cartridge was operated at 25°C.

The background electrolyte (BGE) solution for separation was prepared by first mixing 20 mL of double deionized (DDI) water with the dsDNA 1000 Gel Buffer until the solid gel buffer was fully dissolved. For each 10 mL of gel buffer, 1 µL of SYBR Gold's dye was added and the resulting solution was mixed well by vortexing. The solution was then sonicated to remove any air bubbles.

Results and Discussion

Development of the CE-LIF method for analyzing DNA restriction fragments

To optimize experimental conditions, the effects of various parameters on the resolution of restriction fragments and separation time were tested. The parameters tested included the concentration of separation gel, injection voltage and duration, separation voltage, capillary temperature and length and total separation time.

The effect of gel concentration in BGE on resolution was tested by diluting stock BGE solution 5- or 10-fold using 1X TBE. The overall resolution of the sample decreased with decreasing gel concentration. Next, the impact of injection voltage and duration was investigated. The increase in injection voltage and time led to increases in the amount of sample injected increased, leading to sample overloading and decreased resolution. The effect of separation voltage was examined by increasing this parameter from -7 kV to -15 kV. This manipulation increased separation speed but led to joule heating and decreased resolution. The effect of capillary temperature was then studied by increasing the temperature from 15°C to 30°C. As the capillary temperature increased, the viscosity of the BGE decreased, leading to a decrease in resolution. Finally, the effect of effective capillary length was investigated. We found that capillaries with effective lengths of 30 cm and 40 cm demonstrated similar separation efficiency and resolution. We therefore used capillaries with an effective length of 30 cm to reduce analysis time.

These results indicate that the optimal separation conditions for this application include undiluted BGE, 3 s injection at 0.5 psi, separation voltage of -7 kV, effective capillary length of 30 cm and 25°C capillary temperature. A representative electropherogram obtained under optimized conditions is shown in Figure 2A.

Comparison to agarose gels

Compared to the agarose gel electrophoresis method, CE can better separate the enzyme fragments, resulting in assay results that are more objective and accurate. Figure 2B shows the results obtained by the agarose gel electrophoresis method for the DNA restriction fragment analysis of the genetic material from the HSV vector. Using this method, 7 fragment bands were detected. In contrast, CE-LIF separation shows 8 fragment peaks. Additionally, CE was capable of baseline resolving fragments 4, 5 and 6, despite their poor separation by agarose gel electrophoresis. The CE method detected fragments 7 and 8 in the range above 15 kbp, whereas the agarose gel method only detected fragment 7.

Calculation of the length of DNA restriction fragments

The DNA ladder, DL15000, was analyzed using the optimized CE conditions to obtain 6 fragment lengths, including 1 kbp, 2.5 kbp, 5 kbp, 7.5 kbp, 10 kbp and 15 kbp (Figure 3). The software fitted the data to a linear equation with a linear regression coefficient of 0.99. This linear equation was used to calculate the length of individual fragments in the sample. The results in Table 1 demonstrate that the fragment length results obtained by the CE and agarose gel methods were similar. To calculate the size of the DNA fragments in the sample, the CE software performs linear curve fitting and then calculates the length of restriction fragments based on their migration times.

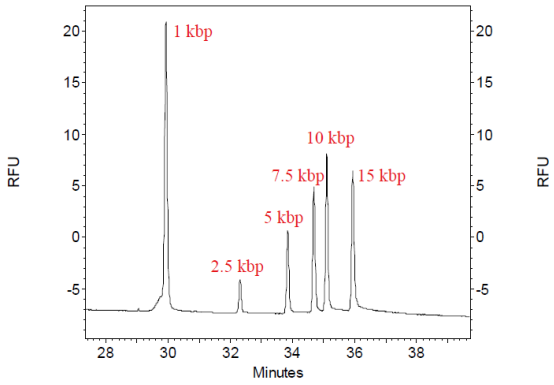

Figure 3. Typical electrophoretic profile of DNA ladder DL15000. The electrophoretic conditions are the same as those used in Figure 2.

Precision experiments

We investigated the precision of the method by injecting the same sample 6 consecutive times using the optimized CE conditions. Table 2 shows that the %RSD of the migration time of each peak is less than 0.32%. Peaks 1 through 7 had %RSD values less than 5.65% for corrected peak area %, while peak 8 exhibited a %RSD value of 12.38%. All peaks demonstrated a %RSD value less than 5.77% for the fragment size calculation. Together, these results indicate that the optimized CE method has good precision.

Table 1. Comparison of the results of the CE-LIF method with the agarose gel method for the determination of DNA fragment length.

Peak #	CE-LIF (kbp)	Agarose gel (kbp)
1	*4.87*	*4.64*
2	*7.20*	*6.72*
3	*8.25*	*8.06*
4	*11.47*	*11.45*
5	*12.91*	*12.85*
6	*14.29*	*14.43*
7	*20.33*	*20.43*
8	*22.19*	*NA*

kbp=kilo base pairs.

Table 2. Precision experiment results (n=6).

Peak #	Migration time (min)		Corrected peak area %		Fragment size (kbp)	
	mean	%RSD	mean	%RSD	mean	%RSD
1	*33.82*	*0.31*	*7.51*	*2.46*	*4.87*	*5.32*
2	*34.54*	*0.31*	*10.66*	*4.64*	*7.20*	*5.77*
3	*34.80*	*0.30*	*22.66*	*3.10*	*8.25*	*5.70*
4	*35.41*	*0.30*	*14.64*	*1.72*	*11.47*	*5.52*
5	*35.64*	*0.30*	*13.68*	*3.31*	*12.91*	*5.60*
6	*35.84*	*0.31*	*13.66*	*2.78*	*14.29*	*5.53*
7	*36.40*	*0.30*	*10.03*	*5.65*	*20.33*	*5.13*
8	*36.76*	*0.32*	*7.11*	*12.38*	*22.19*	*5.18*

Conclusions

- We demonstrated how to optimize a CE-LIF method for the analysis of restriction fragments of nucleic acids in HSV gene therapy products
- Compared to agarose gel electrophoresis, this method demonstrated better resolution, detection of more restriction fragments and accurate calculation of restriction fragment length
- The analysis software enabled a simple and automated method to determine fragment size
- Our data demonstrated the good precision of the assay based on the reproducibility of migration time and corrected peak area %

References

1. Application of the CE-LIF Method to Analyze DNA Restriction Fragments of Recombinant Human Type I Herpes Simplex Virus [J]. Journal of Pharmaceutical Analysis, 2020, 40: 37–42.

Headquarters
500 Old Connecticut Path | Framingham, MA 01701 USA
Phone 508-383-7700
sciex.com

International Sales
For our office locations please call the division headquarters or refer to our website at
sciex.com/offices

Comprehensive method development for a wide size range of RNA

Featuring the PA 800 Plus system and RNA 9000 Purity & Integrity Kit

Mervin Gutierrez, Fang Wang, Quincy Mehta, and Marcia Santos

SCIEX, USA

Introduction

The integrity and quality of the encapsulated nucleic acids used in cell and gene therapy are important to ensure the efficacy and safety of the therapeutic product. Current methods used to characterize the integrity and quality of these nucleic acids are complex and yield suboptimal analytical resolution and poor transferability. This work introduces a new chemistry and methods optimization strategy that is applicable to single-stranded RNAs with lengths ranging from 50 to 9000 bases, enabling scientists to achieve high-resolution and high-quality data (Figure 1). This technical note showcases the reproducibility for electrokinetic injection, a %RSD for migration time below 0.25% and %RSD for corrected peak area% less than 3 for fragments between 300 and 2000 bases for the single-stranded RNA (ssRNA) ladder.

Compared to traditional slab gel-based electrophoresis methods, capillary gel electrophoresis (CGE), combined with laser-induced fluorescence (LIF), offers superior resolution, shorter analysis time, automated operation and exceptional sensitivity. Compared to chip-based CE systems, we demonstrate easy method modification and optimization flexibility, allowing scientists to choose between project-specific methods to achieve optimal results and platform methods for higher throughput.

Capillary Temperature (°C)	Expected Capillary Run Life	Migration Time of 9 kb Peak (min)	Resolution between 7 and 9 kb peaks	EP Theoretical Plates (x 10^6)			
				Peak			
				1 kb	5 kb	7 kb	9 kb
25	130-150	21.18	3.62	1.19	1.37	1.67	1.11
30	100-120	19.78	4.31	1.22	1.98	1.87	1.12
35	70-80	18.51	5	1.24	2.02	1.92	1.39
40	50-60	17.35	5.1	1.22	1.95	1.78	1.39

Figure 1. Summary of assay performance criteria. Capillary run life, migration time for the 9 kb marker as a proxy for total assay time, resolution between 7 kb and 9 kb markers and theoretical plates were evaluated. N = 3 capillaries were evaluated at each temperature.

The SCIEX solution for extended range RNA purity and integrity analysis on the PA 800 Plus system.

This study evaluated an RNA ladder that ranged from 50 to 9000 bases, using the new RNA 9000 Purity & Integrity Kit and the PA 800 Plus system. The effects of varying conditions, such as injection mode and separation temperature, are described.

Key features

- Ready-to-use kit and method for single-stranded nucleic acid analysis
- Easy-to-optimize method strategy for samples containing small or large ssRNA fragments
- Ability to use either hydrodynamic or electrokinetic injections, depending on sample composition, and achieve great resolution
- Ability to separate a wide range of RNAs in a single separation
- Reproducible and reliable results from hydrodynamic injections, with migration time %CV <0.15% and corrected peak area% <4.5%

Methods

Materials: The RNA 9000 Purity & Integrity Kit (PN: C48231), containing the nucleic acid extended range gel, SYBR™ Green II RNA Gel Stain,* acid wash (regenerating solution), CE-grade water, the RNA ladder (50-9,000 bases) and LIF calibration solution, was obtained from SCIEX (Framingham, MA). The Pre-Assembled BFS Capillary Cartridge (30.2 cm bare-fused silica capillary, PN: A55625), SCIEX universal vials (PN: A62251), universal vial caps (PN: A62250) and PCR vials (PN: 144709) were also acquired from SCIEX. The universal vials, universal vial caps and PCR vials were used for sample and reagent loading.

Sample preparation: The RNA 9000 molecular ladder was diluted with SLS, as described in the user manual. Specifically, 4 µL of ssRNA ladder was mixed with 96 µL of SLS. The mixture was then heated at 70°C for 5 minutes using a thermal cycler and immediately cooled on ice for at least 10 minutes. An 80 µL aliquot of the sample was transferred into the sample vial before being subjected to sample analysis.

Instrument and software: The PA 800 Plus system (SCIEX), equipped with a laser-induced fluorescence (LIF) detector with a 488 nm solid-state laser and a 520 nm emission filter, was used for all separations. The LIF detector was calibrated according to the user guide. Data acquisition was performed using 32 Karat software version 10. Data files were exported in the ASCII format and later imported and processed using the BioPhase software to perform integration and calculations of signal intensity, corrected peak area and corrected peak area%.

Instrument set-up: The separation gel was prepared by mixing 10 µL of SYBR™ Green II RNA Gel Stain* with 5 mL of nucleic acid extended range gel. This separation gel was used for 8 injections, but this preparation can be scaled to the number of samples to be analyzed. The separation gel was prepared at the time of the experiment and leftover gel was discarded. The PA 800 Plus universal vials were then filled with 1.5 mL of separation gel and all other reagents needed for this application. The vials were properly capped before they were loaded onto the instrument, according to the reagent plate map provided in the user guide.[1] The separation method can be downloaded from the SCIEX website or created following the user guide.[1] For separation temperature screening, the capillary cartridge temperature was set to various temperatures between 25°C and 55°C for the pressure injection methods.

Results and Discussion

Effect of separation temperature

Separation temperature is an important consideration for CE method development. Higher temperatures can speed up the run time and affect peak resolution and shape. The PA 800 Plus system provides an accurate temperature control system that allows the user to set, evaluate and control the separation temperature to achieve an optimal balance of assay throughput and separation efficiency. Here, we assessed the separation of the ssRNA ladder with a size range of 50 to 9000 bases as a function of temperature. The overlaid electropherograms shown in Figure 2 show that separation time is reduced as the separation temperature increases. This result was expected, as an increase in temperature reduces the viscosity of the sieving matrix of the separation gel. Notably, the separation temperature also affected the resolution of the ssRNA markers in a manner dependent on the ssRNA fragment size. Higher temperatures improved the resolution of the larger RNA markers, whereas lower temperatures improved the resolution of the smaller RNA markers (Figure 1). Figure 3 shows the scatter plot of migration time, theoretical plates and peak widths for each of the ssRNA markers as a function of the separation temperature.

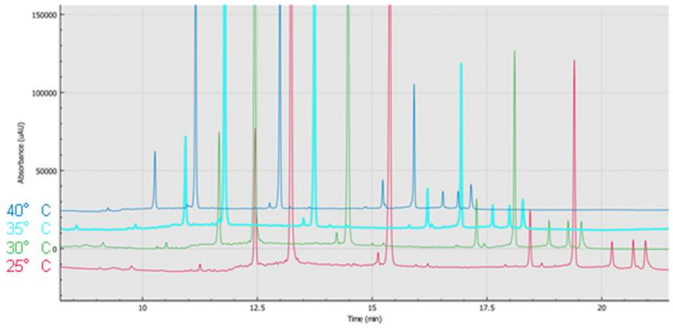

Figure 2. Overlaid ssRNA ladder electropherograms to compare separation at different temperatures. As the temperature increases, the migration time decreases and peak resolution is affected for all markers. Further details and quantitative comparison are presented in Figure 3. The capillary cartridge temperatures tested included 25°C, 30°C, 35°C and 40°C, from the bottommost to topmost electropherogram.

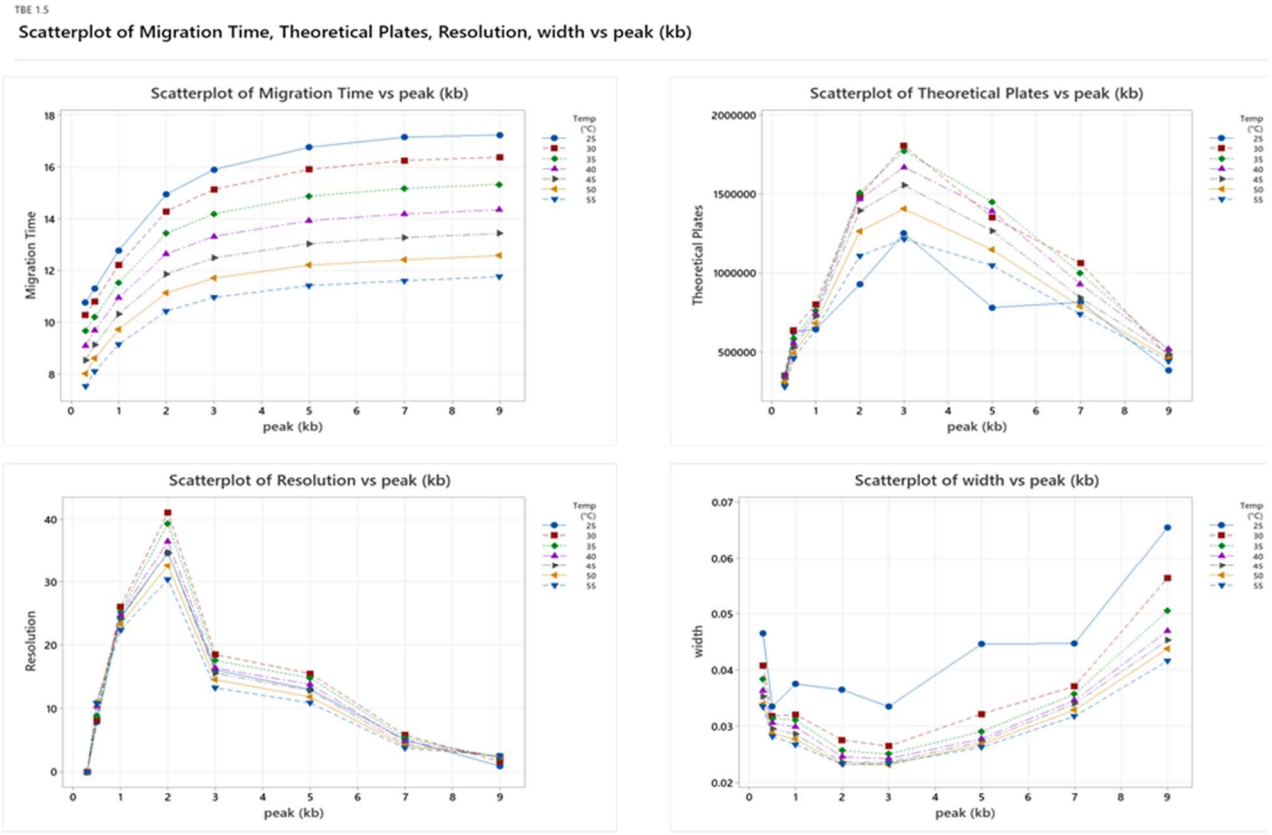

Figure 3. Quantitative analysis of ssRNA marker separation performance. Scatter plots of theoretical plates, peak resolution, peak width and migration time for all RNA markers at 7 different temperatures. Temperatures tested included 25°C (blue circle), 30°C (red square), 35°C (green diamond), 40°C (pink upward-facing triangle), 45°C (purple right-facing triangle), 50°C (yellow left-facing triangle) and 55°C (blue downward-facing triangle).

Interestingly, we found that increased separation temperature might detrimentally impact separation performance over time. N=3 cartridges were evaluated at temperatures between 25°C and 40°C to establish the optimal operation limit to preserve capillary longevity. Analysis revealed that 30°C is the best separation temperature to both maximize the run life of the capillary and resolve fragments that are in a size range of potential therapeutic relevance, between 1000 and 9000 bases.

Evaluation of injection modes

Either hydrodynamic (HDI) or electrokinetic (EKI) injections can be performed with the RNA 9000 Purity & Integrity Kit. For the HDI mode, pressure is used to drive a small volume of sample into the capillary, whereas for the EKI mode, an electric field is used to drive only the charged species of the sample into the capillary. EKI mode uses reverse polarity in CGE, in which residual electro-osmotic (EOF) flow moves away for the detector. As a result, only anionic species are introduced into the capillary. The different means by which sample is introduced to the capillary between these 2 methods results in HDI being representative of all sample components and EKI being biased towards species in the sample with higher mobility.[4] Figures 4 and 5 showcase the typical profile of ssRNA ladder using HDI and EKI modes, respectively.

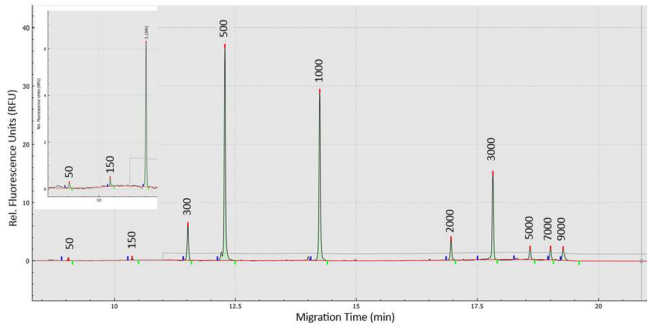

Figure 4. Separation results from the HDI method. Electropherogram of ssRNA ladder analyzed using HDI mode at 1psi for 5 seconds. The inset shows the y-axis zoom-in for markers smaller than 300 bases. Testing was performed on a 20/30 cm, 50 µm ID BFS capillary at 30°C capillary temperature and 200 V/cm field strength.

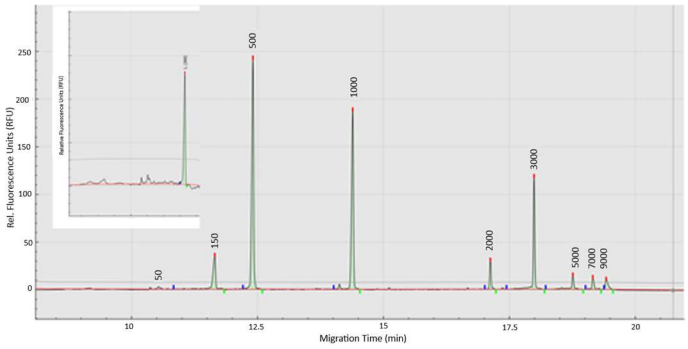

Figure 5. Separation results from the EKI method. Electropherogram of ssRNA ladder analyzed with EKI at 5 kV for 3 seconds. The inset shows the y-axis zoom-in for markers smaller than 300 bases. Testing was performed on a 20/30cm 50 µm ID BFS capillary at 30°C capillary temperature and 200 V/cm field strength.

The results indicated that both HDI and EKI modes yield similar profiles for markers larger than 300 bases. We observed increased peak widths of fragments between 50 and 300 bases using the EKI mode, but not HDI mode. The increase in peak widths results in decreased theoretical plates and might have a negative impact on the ability to assess purity fragments with sizes between 50 and 150 bases. Therefore, a pressure injection should be considered if the analyte of interest is smaller than 300 bases. Conversely, EKI is inherently a stacking technique because it induces a pre-concentration of the sample band during the injection, resulting in this case, in a 5-fold increase in response signal. Furthermore, EKI mode is recommended when working with samples present at low concentrations and containing RNA fragments above 300 bases.

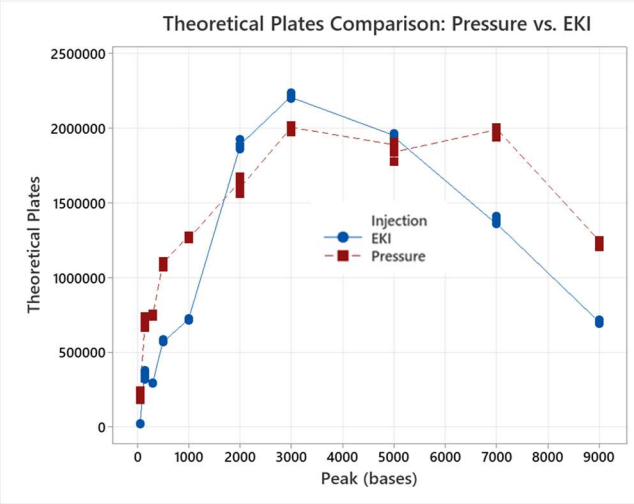

Figure 6. Comparison of theoretical plates for each ssRNA marker using EKI and HDI. The EKI method (blue circle) was implemented at 5 kV for 3 seconds and the HDI method (red square) was implemented at 1psi for 5 seconds. Testing was performed on a 20/30cm 50 µm ID BFS capillary at 30°C capillary temperature and 200 V/cm field strength.

It is possible to impart stacking capability to the HDI mode by injecting a small water plug before the injection of the sample. This technique allows for a significant improvement in peak shape and resolution for the ssRNA fragments smaller than 300 bases. A quantitative evaluation of the theoretical plates between EKI and HDI modes is shown in Figure 6. Based on these factors, HDI is recommended for analytes smaller than 500 bases.

Assay repeatability

The repeatability of the method was evaluated at 30°C separation temperature for the 2 injection modes. Sixteen injections were performed for each prepared sample, using EKI (Figure 7) or HDI (Figure 8). The average and %RSD for migration time and corrected peak area were calculated for each fragment size marker peak. Only fragments larger than 300 bases were considered in the calculations for the EKI mode (Table 1), whereas all 10 fragment markers were evaluated for the HDI mode (Table 2).

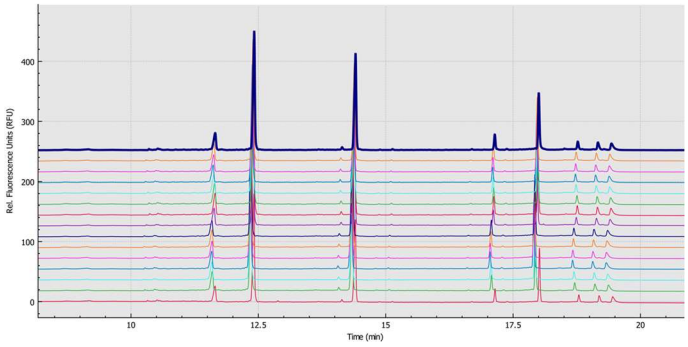

Figure 7. Assay repeatability using the EKI method. Overlaid electropherograms of 16 ssRNA ladders analyzed with the EKI method at 5 kV for 3 seconds. Testing was performed on a 20/30cm 50 µm ID BFS capillary at 30°C capillary temperature and 200 V/cm field strength.

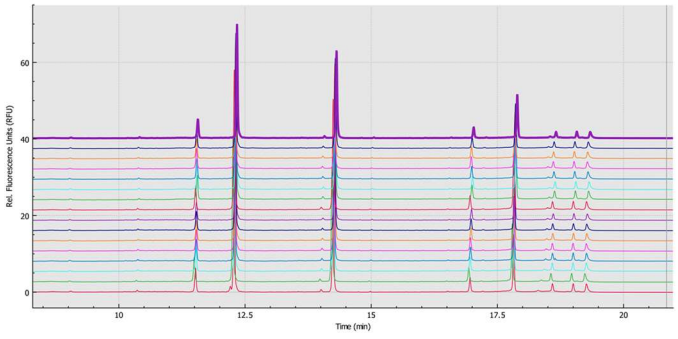

Figure 8. Assay repeatability using the HDI method. Overlaid electropherograms of 16 ssRNA ladders analyzed with the HDI method at 1 psi for 5 seconds. Testing was performed on a 20/30cm 50 µm ID BFS capillary at 30°C capillary temperature and 200 V/cm field strength.

Table 1. Repeatability evaluation of the EKI mode for separation of ssRNA ladders.

Peak ID	300	500	1000	2000	3000	5000	7000	9000
Average for MT	*11.62*	*12.38*	*14.37*	*17.10*	*17.96*	*18.72*	*19.12*	*19.39*
%RSD for MT	*0.23*	*0.20*	*0.18*	*0.18*	*0.19*	*0.19*	*0.19*	*0.19*
Average for corrected peak area%	*8.96*	*40.46*	*29.15*	*3.04*	*11.93*	*2.62*	*1.91*	*1.93*
%RSD for corrected peak area%	*7.20*	*1.54*	*2.30*	*7.46*	*4.00*	*9.62*	*10.99*	*6.42*

Table 2. Repeatability evaluation of the HDI mode for separation of ssRNA ladders.

Peak ID	50	150	300	500	1000	2000	3000	5000	7000	9000
Average for MT	*9.03*	*10.38*	*11.54*	*12.31*	*14.27*	*16.98*	*17.84*	*18.61*	*19.02*	*19.28*
%RSD for MT	*0.09*	*0.15*	*0.15*	*0.15*	*0.15*	*0.13*	*0.13*	*0.13*	*0.13*	*0.13*
Average for corrected peak area%	*0.48*	*0.54*	*7.77*	*40.59*	*30.07*	*3.10*	*11.70*	*2.15*	*1.51*	*2.09*
%RSD for corrected peak area%	*10.56*	*4.82*	*1.86*	*1.43*	*1.74*	*1.44*	*1.24*	*4.24*	*2.00*	*2.71*

When EKI mode was used, the migration time of the fragment markers increased slightly (Figure 7), resulting in minimum impact to the %RSD for migration time <0.25%. Due to the small contribution of the markers at 50 and 150 bases to the total corrected peak area, the reported corrected peak area% for markers above 300 bases is not affected when the different injection modes are used. The separations using EKI mode show a higher %RSD for corrected peak area% for each marker, possibly due to the inherent bias introduced by EKI.[4] The average total corrected peak area for the pressure injection was 4.52, compared to 34.99 for the EKI injection, which is consistent with the increased sample load typical of an EKI injection.

Conclusions

- The RNA 9000 Purity & Integrity Kit provides high-resolution separation for RNAs ranging from 50 to 9000 bases
- The method can be easily optimized and tailored to different RNA sizes, assay requirements and sample matrices by adjusting separation temperature and injection mode
- The assay showed high repeatability and consistency under the conditions evaluated

References

1. RNA 9000 Purity & Integrity Kit Application Guide, for the PA 800 Plus Pharmaceutical Analysis System
2. Julia Khandurina, Hur-Song Chang, Bart Wanders, and Andras Guttman, Automated high-throughput RNA analysis by capillary electrophoresis, BioTechniques 32:1226-1230, 2002
3. CMC Considerations for mRNA Based Therapeutics, Intertek
4. Capillary Electrophoresis: Theory and Practice, Second Edition, 1992, Paul D. Grossman and Joel C. Colburn, Elsevier Science & Technology Books

Headquarters
500 Old Connecticut Path | Framingham, MA 01701 USA
Phone 508-383-7700
sciex.com

International Sales
For our office locations please call the division headquarters or refer to our website at
sciex.com/offices

Characterization of oligonucleotides and related impurities to support the development of drug substances

Find, relatively quantify, and confirm the structure of oligonucleotides and their impurities using the SCIEX ZenoTOF 7600 system and Molecule Profiler software

Remco van Soest, Kerstin Pohl, Yunyun Zou and Elliott Jones
SCIEX, USA

This technical note describes the identification, relative quantification and structural confirmation of oligonucleotides and related impurities. Relative quantification and full sequence coverage was achieved at levels as low as 0.3% (*w/w*).

Oligonucleotide therapeutics and gene therapies are rapidly gaining attention as their potency improves and delivery challenges are addressed. Modalities such as antisense oligonucleotides (ASOs) are becoming more important due to their high specificity and ability to reach formerly undruggable targets. To ensure safe drugs, methods for the identification and characterization of the full length product (FLP) and impurities are critical. High resolution mass spectrometry (HRMS) can be used for the identification of potential impurities, by comparing the measured accurate masses and isotope patterns with those calculated. However, there is a lack of powerful yet intuitive processing software, and manual interpretation is cumbersome and time consuming. Furthermore, structural confirmation leveraging MS/MS adds an additional level of complexity.

Using the Molecule Profiler software to overcome these challenges, this technical note shows the identification and relative quantification of the 5'(*n*-1), 5'(*n*-2) and 5'(*n*-3) impurities of a fully phosphorothioated FLP spiked into an FLP sample at levels between 0.1 and 10% (w/w). The software can perform relative quantification based on TOF-MS, and assign fragment ions of the potential impurities to confirm their structures, facilitating the characterization of drugs in development.

Key features of Molecule Profiler software for oligonucleotide impurity analysis

- Excellent quality and high mass accuracies for TOF-MS and TOF-MS/MS data allow for confident assignment of oligonucleotide FLP and impurities in Molecule Profiler software
- Straightforward quantification based on TOF-MS peak areas can be achieved by grouping of charge states or alternatively UV data can be leveraged for quantification
- Significant improvement of identification of low abundant impurities by boost in S/N and increased fragment assignment using the Zeno trap

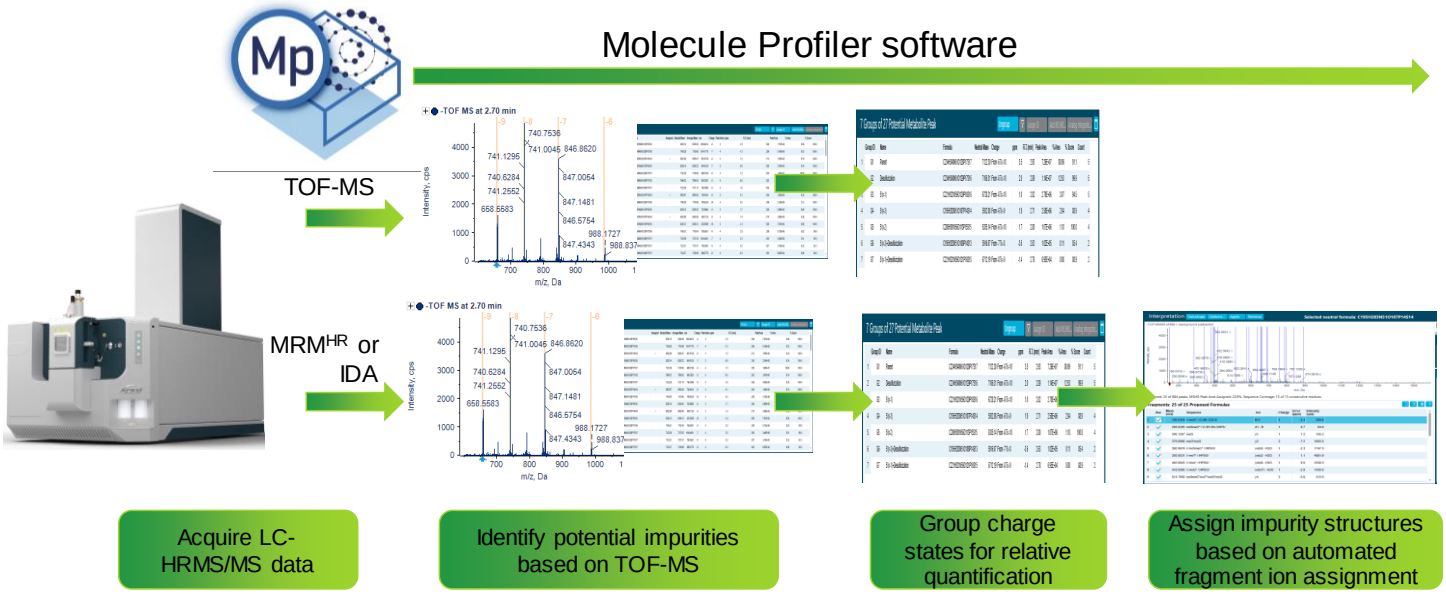

Figure 1. Workflow representation for relative quantification and structural confirmation of impurities using the Molecule Profiler software.

Methods

Samples and reagents: A 18-mer 2'-O-methoxyethyl phosphorothioated oligonucleotide with the same sequence as nusinersen, a drug developed for the treatment of spinal muscular atrophy, and its 5'(*n*-1), 5'(*n*-2) and 5'(*n*-3) impurities were ordered (desalted) from IDT. The ion-pairing reagents 1,1,3,3,3-hexafluoroisopropanol (HFIP, ≥ 99.8%) and diisopropylethylamine (DIEA, ≥ 99.5%,), and ethylenediaminetetraacetic acid (EDTA), were purchased from Sigma Aldrich.

Sample preparation: Samples of 10 µg/mL FLP in mobile phase A containing 100 µM EDTA were spiked with the three related shortmers at 0.1, 0.3, 1, 3 and 10% (*w*/*w* relative to FLP) in order to mimic process-related impurities. The FLP was used as a control sample.

Chromatography: A Shimadzu LC-20 series HPLC system was used with water as mobile phase A and 90:10 methanol/water (*v*/*v*) as mobile phase B, both with 15 mM N,N-diisopropylethylamine and 35 mM hexafluoroisopropanol. A gradient from 20-40% B in 5 min with a 1.5 min wash step at 90% B was used at a flow rate of 0.25 mL/min. The column was a Waters ACQUITY PREMIER Oligonucleotide C18 (2.1 × 50 mm, 1.7 µm, 130 Å) at 70ºC, and the injection volume was 10 µL.

Mass spectrometry: A SCIEX ZenoTOF 7600 system was used in negative polarity using an MRM^{HR} method (method details available on request). To determine the precursor masses, the data from a TOF-MS scan of the 10% spiked sample was processed using the Molecule Profiler software to extract the *m*/*z* values for the most abundant charge states for the FLP, the spiked-in impurities, and the desulfurization products (back-exchange of one S to O) of each of these. Collision-induced dissociation (CID) was used, and collision energies (CE) were selected that ensured the generation of fragment rich MS/MS spectra. The parameters for the final MRM^{HR} method are summarized in Table 1. The Zeno trap is located before the TOF pulser and accumulates ions during each TOF pulse, resulting in up to 90% duty cycle. Data was acquired both with Zeno trap on and off, to determine the effect of the Zeno trap functionality on MS/MS data quality.

Table 1. MS parameters.

Parameter	MS	MS/MS
Scan mode	*TOF-MS*	*MRM^{HR}*
Polarity	*negative*	
Gas 1	*70 psi*	
Gas 2	*70 psi*	
Curtain gas	*30 psi*	
Source temperature	*350°C*	
Ion spray voltage	*-4000 V*	
Declustering potential	*-80 V*	
CAD gas	*7*	
Start mass	*600 m/z*	*150 m/z*
Stop mass	*2,000 m/z*	*3,000 m/z*
Q1 resolution	*NA*	*Low*
Accumulation time	*0.1 s*	*0.03 s*
Collision energy	*-10 V*	*available upon request*
CE spread	*0 V*	*3 V*
Zeno trap	*NA*	*ON/OFF*
ZOD threshold (CID)	*NA*	*40,000 cps*
Time bins to sum	*6*	*12*
QJet RF amplitude	*190 V*	*190 V*

Data processing: Data was processed using the SCIEX Molecule Profiler software. Considering the structure of the oligonucleotide, the number of bonds to break in the parent structure, and a comprehensive list of 83 possible standard transformations, the software identifies the different charge states of potential impurities. This assignment is based on the accurate mass match - a 20 ppm tolerance was used for the work presented in this application note - and the match between the measured and theoretical isotope patterns. Additional transformations can be added, while also custom nucleotide residues can be used by defining the 5' and 3' linkers, sugar, base and phosphate groups (Figure 2). The list of found potential impurities can be manually curated, and the different charge states of each potential impurity are grouped together for relative quantification based on the TOF-MS data.

For confirmation of the structure of each potential impurity, MS/MS spectra can be automatically annotated with *a*, *a*-B, w, *b*, *x*, *c*, *y* and *d* fragments (see Figure 2). Sequence coverage by consecutive fragments is automatically calculated by the software.

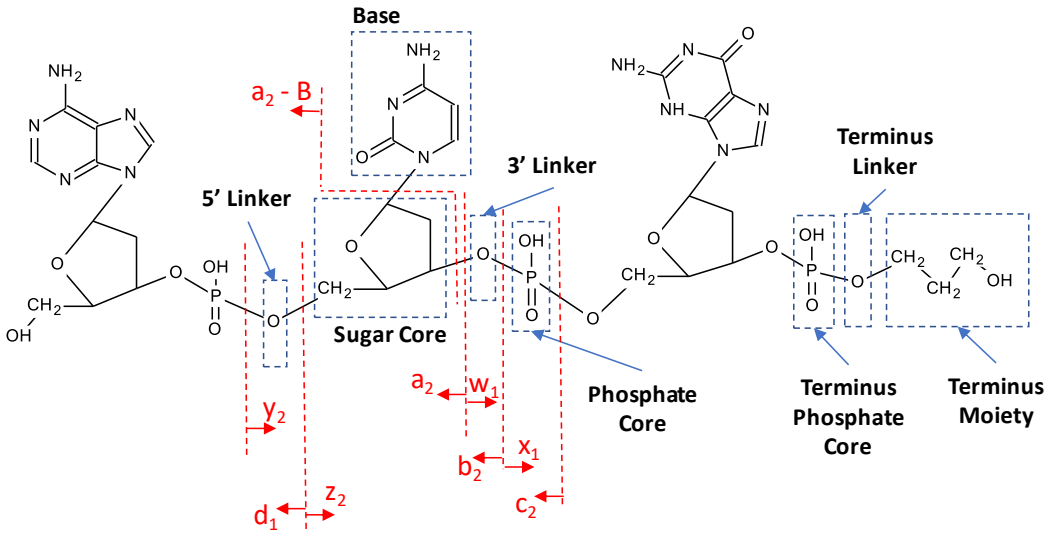

Figure 2. Representation of an oligonucleotide showing the different groups that can be defined for custom nucleotides. Also, the nomenclature of the MS/MS fragments used for sequence confirmation is shown in this figure, taken from the Molecule Profiler software.

Chromatography

Impurities of oligonucleotides are difficult to baseline separate from the main product with reversed phase LC while providing medium to high throughput, especially if they differ only by one or two nucleotides. Modified backbones such as phosphorothioated species are essential for improved pharmacokinetic properties and binding to the target, but complicate separation even further because they are mixtures of diastereomers, resulting in peak broadening. Figure 3 shows the separation achieved for the three spiked in impurities; only the 5'(*n*-3) showed (partial) separation from the FLP.

Relative quantification

Samples of 10 µg/mL FLP spiked with the three 5' deletion impurities at 0.1, 0.3, 1, 3 and 10% (*w/w*) levels were measured and analyzed using the Molecule Profiler software. Processing parameters (Figure 4) were selected to allow for the identification of the FLP and the impurities. Based on the TOF-MS data, the FLP and potential impurities are being matched to the different charge states (see *n*-3 impurity matching in Figure 5). All identified charge states can be easily grouped for an automatic calculation of the %area for the main component and each potential impurity. The %area is the sum of the TOF-MS areas of all found charge states of each identified analyte as a percentage of the total area of all analytes found. In Table 2 the %areas of the spiked-in impurities are listed for each of the spike-in levels. The purity found for the control sample is consistent with the information from the manufacturer for products that have not been purified with HPLC.

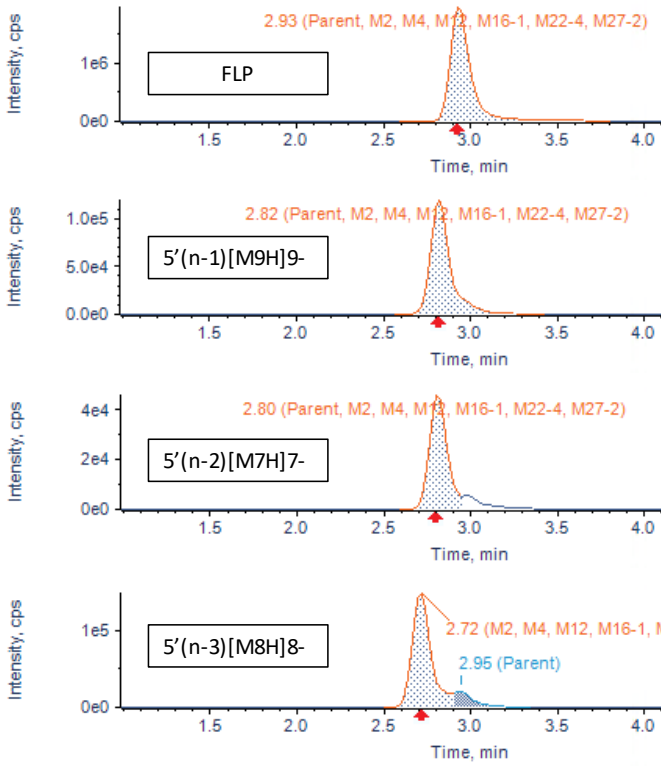

Figure 3. XICs of one charge state for the FLP and each of the spiked-in impurities generated in Molecule Profiler software. (Partial) separation from the FLP was only achieved for the 5'(*n*-3) impurity.

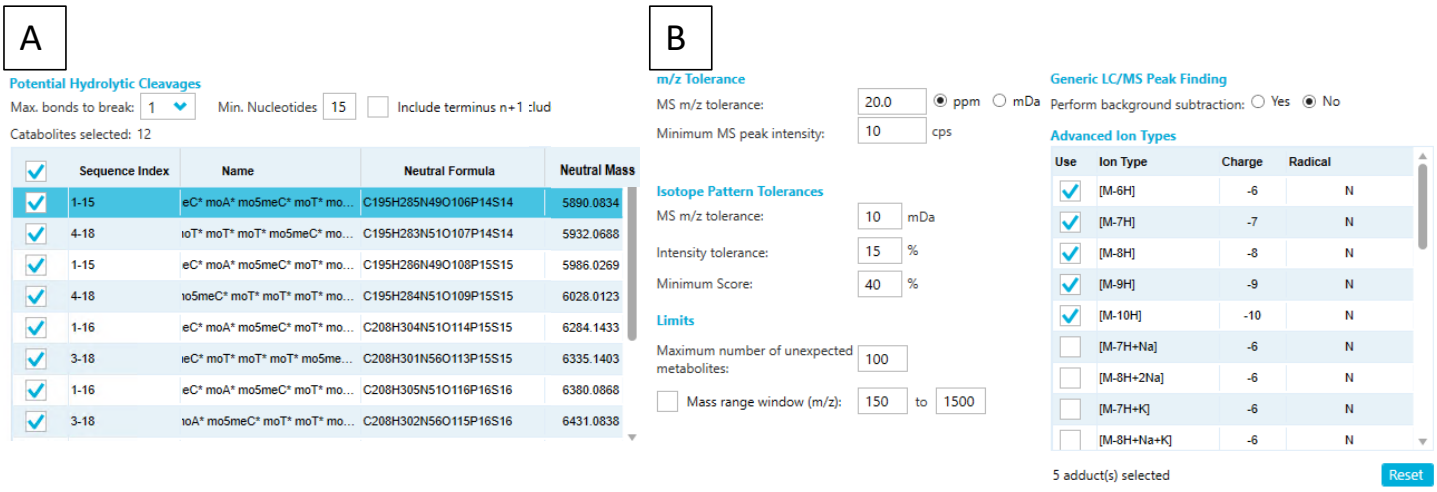

Figure 4. Main settings used for the identification of potential impurities based on the TOF-MS data. A:The search space was limited to impurities with a maximum of one bond broken and a minimum length of 15 nucleotides (the FLP contained 18 residues). No internal *n*-1 or terminal *n*+1 impurities were searched for, as the main objective of this study was to demonstrate the capability of the software to find the spiked-in 5' *n*-1 to *n*-3 shortmers. B: An MS *m*/*z* tolerance of 20 ppm was used, and charge states -6 to -10 were considered.

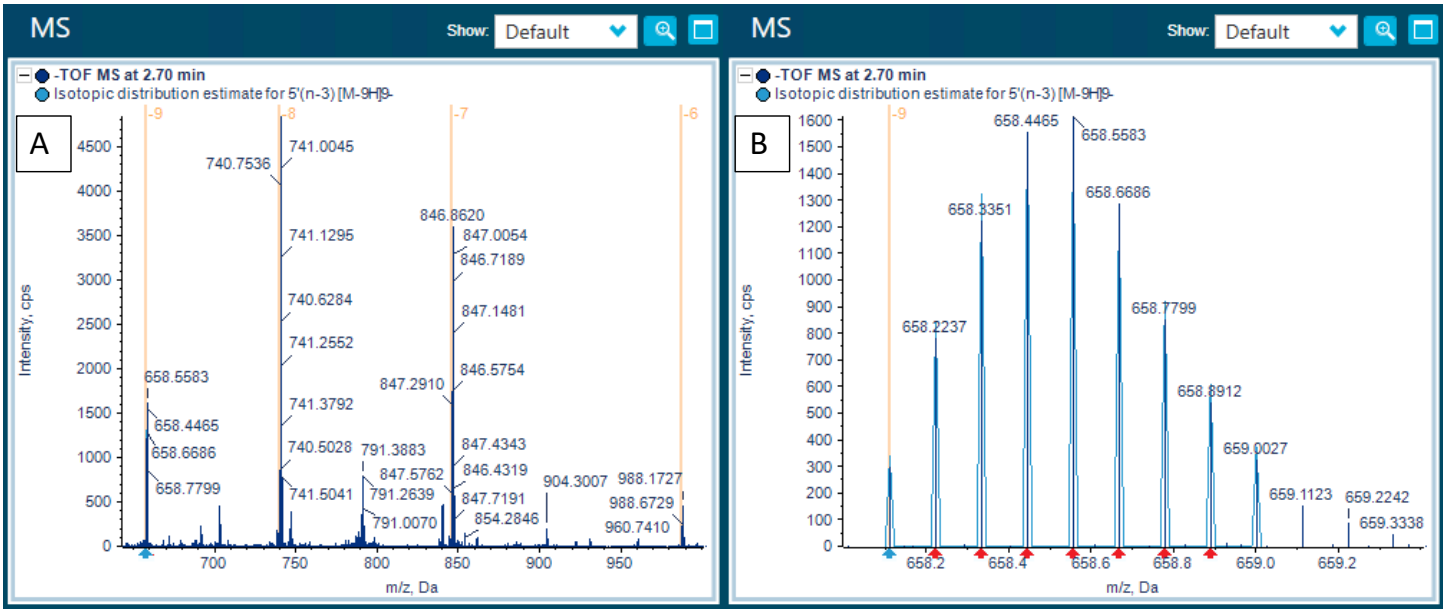

Figure 5. Identification of potential impurity based on the TOF-MS data. A:TOF-MS showing identified charge states (yellow labeling) and suggested ID for the 5'(*n*-3) at 3% spike-in level. B: Zoom-in to TOF-MS data of charge state -9 for 5'(*n*-3). Blue arrow indicates the theoretical monoisotopic mass and the first seven isotopes are indicated with red arrows. An overlay of the theoretical isotopic distribution can be used for confidence in the correct assignment.

The main impurities found in the control sample were desulfurization (12.7%), and di-desulfurization (0.78%). Correlation between the spiked in amounts, and the reported relative areas was good for the 5'(*n*-1) and 5'(*n*-3) impurities, with small amounts found in the control sample. For the 5'(*n*-2) impurity the correlation was found to be poor. Upon further inspection of the data, this could be attributed to an overlap of the -8 charge state isotopes of the impurity with those of the -9 charge state of the drug. For relative quantification of this impurity based on MS data, a better chromatographic separation will be required. Alternatively the Analytics module in SCIEX OS software can be used to accurately quantify this impurity based on reconstruction of the TOF-MS data, or by quantification based on fragment masses using MRM^{HR} data. Note that the Molecule Profiler software also supports relative quantification based on UV data (not shown).

Table 2. Relative quantification of the spiked-in impurities. The %areas are based on the summed areas of all identified charge states of an impurity relative to the area of all identified peaks.

Spike-in (% w/w of FLP)	Spike-in (% w/w of total)	FLP (% area)	*n*-1 (%area)	*n*-2 (%area)*	*n*-3 (%area)
0	*0.00*	*83.01*	*0.11*	*NA*	*0.26*
0.10	*0.10*	*82.5*	*0.17*	*0.02*	*0.34*
0.30	*0.30*	*80.99*	*0.34*	*0.11*	*0.50*
1.00	*0.97*	*81.34*	*0.97*	*0.37*	*1.08*
3.00	*2.75*	*75.48*	*2.89*	*1.12*	*2.68*
10.00	*7.69*	*63.35*	*8.73*	*6.39*	*8.73*

* Because of an overlap of the -8 charge state isotopes of the 5'(*n*-2) impurity with the -9 charge state of the FLP (no chromatographic resolution), the charge state was excluded for relative quantification, leading to lower %area values for the 5'(*n*-2) impurity.

Correlation

The Molecule Profiler software also allows for comparing the peak areas of impurities between different samples. This feature of the software could be used to, for example, compare products that are purified using different methods, or track product quality. In Figure 6 this function of the software was used to graph the peak areas for the 5'(*n*-1) and the 5'(*n*-3) impurity for the different spike-in levels.

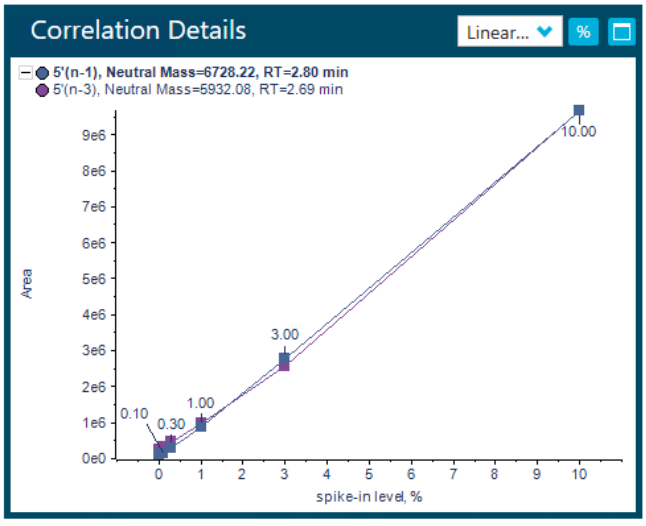

Figure 6. Correlation plot of area vs. %spike-in. Plots for the 5'(*n*-1) and 5'(*n*-3) impurities with good linearity are shown.

Structural confirmation

The potential impurities the software suggests are based on accurate mass and isotope pattern matching of the TOF-MS data. The location of a modification, or the actual position of all nucleotides in an impurity cannot be determined with MS only.

As the structure of an impurity can be important for its potential toxicity, confirming the correct structures is critical. The Molecule Profiler software can help in confirming the structures of each of the potential impurities by annotating the MS/MS spectra acquired for their different charge states. Allowing for *a*, *w*, *c*, y and *d* terminal fragments, and allowing for the loss of one base or water molecule, the Molecule Profiler software was used to annotate the different charge states and calculate the consecutive sequence coverage with an *m*/*z* tolerance of 10 ppm. Figure 7 shows an example of the number of consecutive residues being identified in the MS/MS data for all charge states combined for the 5'(*n*-3) impurity at the various spike-in levels. Full coverage was found for all except the lowest spike-in level (0.10%) when the Zeno trap functionality was used. Without the Zeno trap, the coverage was significantly lower, as expected. Figure 8 provides a comparison of how much more information-rich MS/MS spectra with higher S/N can be acquired using the Zeno trap versus without it.

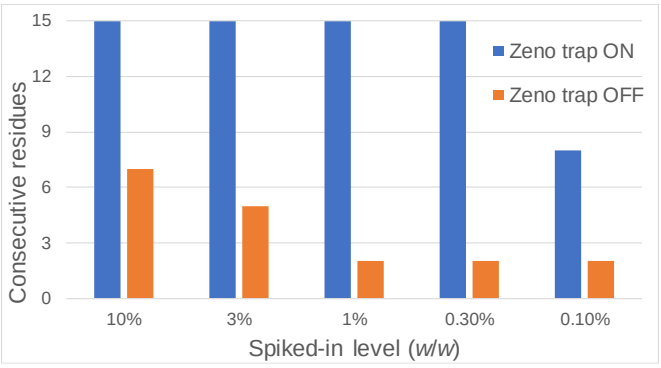

Figure 7. Consecutive residues for different spiked-in levels of the 5'(*n*-3) impurity, with and without use of the Zeno trap. The impurity has a length of 15 nucleotides.

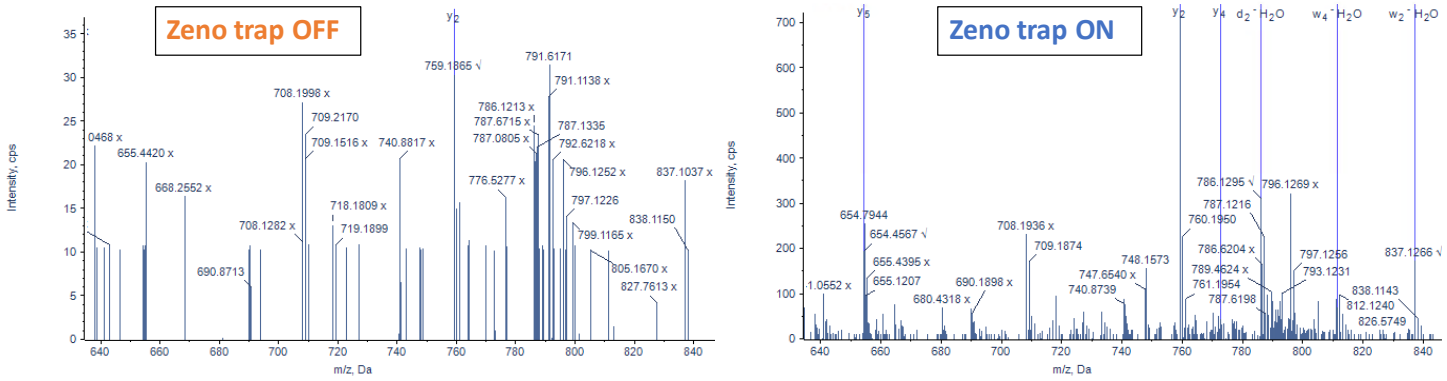

Figure 8. Zoom-in to the MS/MS spectrum of the 5'(*n*-3) impurity -8 charge state at the 0.3% spiked-in level. Data was acquired without using the Zeno trap (left) and with using the Zeno trap (right). Only one fragment ion was found in the MS/MS spectrum acquired without using the Zeno trap. S/N of the spectrum with Zeno trap on was approximately 10x better, showing significantly more automatically assigned fragment ions in Molecule Profiler software.

The higher quality data when using the Zeno trap therefore resulted in the software finding many more fragments. Figure 9 shows an example of identified fragment ions in the MS/MS spectra from an impurity. This information can be used to confirm the identification based on TOF-MS even further.

Fragments: 10 of 36 Proposed Formulae

Use	Mass (m/z)	Sequence	Ion	Charge	Error (ppm)	Intensity (cps)
☑	340.1269	moG	y1	1	1.9	190.8
☑	379.0892	moG*moG	y2	2	-9.2	123.6
☑	759.1913	moG*moG	y2	1	-1.9	5771.0
☑	576.1206	moT*moG*moG	y3	2	-3.6	1462.0
☑	1153.2532	moT*moG*moG	y3	1	0.4	67.5
☑	514.7696	mo5meC*moT*moG*moG	y4	3	-3.4	162.2
☑	772.6577	mo5meC*moT*moG*moG	y4	2	-3.8	241.1
☑	654.4588	moG*mo5meC*moT*moG*moG	y5	3	-2.1	898.8
☑	689.8710	moA*moT*moG*mo5meC*moT*moG*moG	y7	4	-7.6	197.3
☑	790.6429	moA*moA*moT*moG*mo5meC*moT*moG*moG	y8	4	-1.6	95.8

Figure 9. Example of the annotation table in the Molecule Profiler software. The table shows the proposed fragments for a particular *m/z*, their charge states, mass accuracies and intensities. The data is from the 5'(*n*-3) impurity -8 charge state at the 3% spiked-in level, acquired using the Zeno trap .Only the *y* fragments are shown.

Conclusions

- Excellent TOF-MS data quality and mass accuracy were leveraged for the identification of FLP and spiked-in impurities down to a 0.3% level
- A fast and accurate relative quantification of oligonucleotides and their impurities based on TOF-MS or UV data can be performed in Molecule Profiler enabling fast product quality control
- The annotation of TOF-MS/MS with the most commonly found fragment ions based on a proposed structures in Molecule Profiler software greatly reduces manual workload and speeds up the correct identification of oligonucleotide-based drugs and impurities
- TOF-MS/MS data quality and fragment assignment can significantly be enhanced using the Zeno trap with the ZenoTOF 7600 system, which allows for the identification of even very low abundance impurities

Headquarters
500 Old Connecticut Path | Framingham, MA 01701 USA
Phone 508-383-7700
sciex.com

International Sales
For our office locations please call the division headquarters or refer to our website at
sciex.com/offices

Identification and relative quantification of oligonucleotide metabolites from extracted rat plasma

Identify and confirm the structure of oligonucleotide metabolites using the X500B QTOF system and Molecule Profiler software from SCIEX

Remco van Soest, Kerstin Pohl and Todd Stawicki
SCIEX, USA

This technical note describes the identification, relative quantification and structural confirmation of 9 metabolites of an oligonucleotide spiked in a rat plasma extract.

Oligonucleotide therapeutics and gene therapies are rapidly gaining attention as their potency improves and delivery challenges are addressed. Modalities such as antisense oligonucleotides (ASOs) are becoming more important due to their high specificity and ability to reach formerly undruggable targets. To ensure safe drugs, methods for the identification and characterization of the full-length product (FLP) and metabolites are critical. Accurate mass spectrometry (MS) can be used for the identification of potential metabolites, by comparing the measured *m/z* and isotope patterns with those calculated. However, there is a lack of powerful yet intuitive processing software and manual interpretation is cumbersome and time consuming. Furthermore, structural confirmation leveraging MS/MS adds an additional level of complexity.

Using the Molecule Profiler software to overcome these challenges, this technical note shows the identification and relative quantification of 9 potential metabolites of a fully phosphorothioated and partially 2'-O-(2-methoxyethylated) and 5-methylated FLP spiked into a plasma extract at 3% (*w/w*). The software can perform relative quantification based on TOF MS and assign MS/MS fragment ions of potential metabolites to confirm their structures, facilitating the characterization of drugs in development (Figure 1).

Key features of the SCIEX X500B QTOF system and Molecule Profiler software for oligonucleotide metabolite analysis

- Excellent data quality and high mass accuracies for TOF MS and TOF MS/MS data allow for confident assignment of oligonucleotide FLP and metabolites using the Molecule Profiler software
- Straightforward relative quantification based on TOF MS peak areas is achieved by grouping charge states considering all isotopes for highest accuracy
- Fragment coverage displays of proposed sequences based on MS/MS data enable confident identification of metabolites based on user selectable fragment ion types

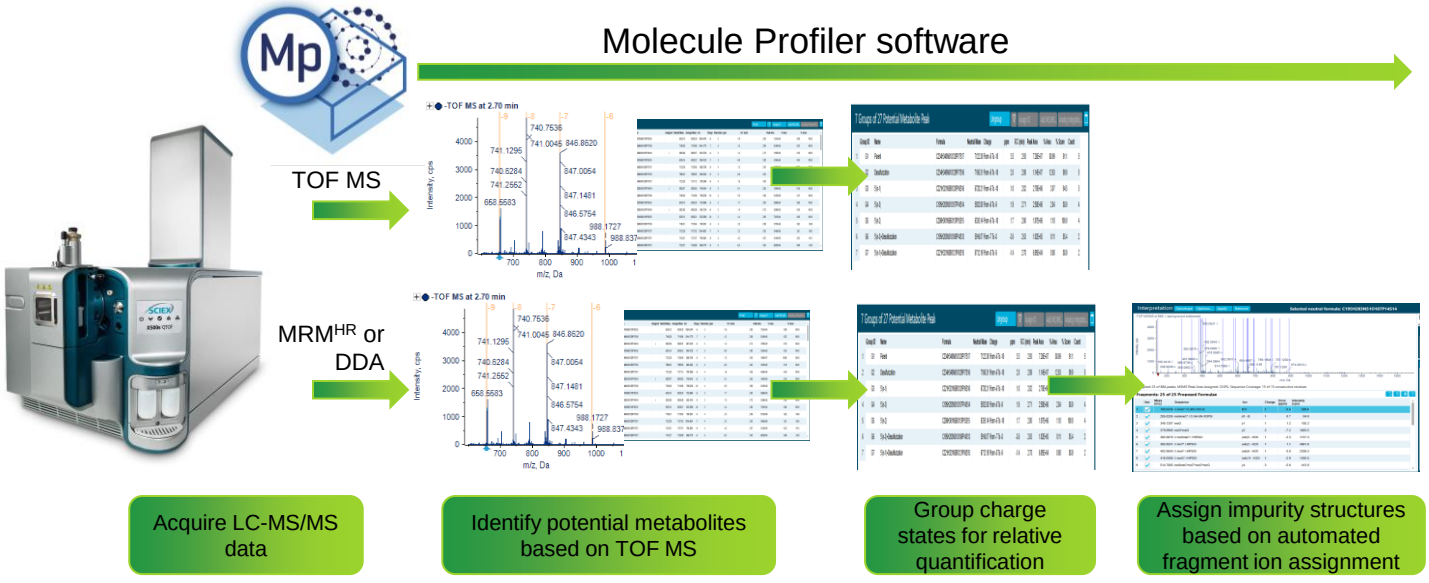

Figure 1. Workflow representation for relative quantification and structural confirmation of metabolites using the Molecule Profiler software.

Methods

Samples and reagents: A 20-mer fully phosphorothioated oligonucleotide with 2'-O-methoxyethyl and 5-methyl modifications (ASO-20PS2MOE-FLP) that has the same sequence as mipomersen, a drug developed for the treatment of familial hypercholesterolemia via RNAseH-mediated degradation of apoB-100 mRNA, was used as the FLP. To simulate metabolites, the 5'(*n*-1), (*n*-2) and (*n*-3) shortmers and 6 metabolites identified in the literature (see Table 1) were used.[1] All oligonucleotides were ordered (desalted) from IDT. The ion-pairing reagents 1,1,3,3,3-hexafluoroisopropanol (HFIP, ≥99.8%) and diisopropylethylamine (DIEA, ≥99.5%,) were purchased from Sigma Aldrich.

Sample preparation: 1 mL rat plasma was extracted using Clarity OTX solid phase extraction (SPE) cartridges (Phenomenex) following the manufacturer's protocol for extracting oligo therapeutics from biological samples. After drying with nitrogen gas at 40°C, the plasma extract was reconstituted in 1 mL mobile phase A. Samples of 20 µg/mL FLP and of the FLP plus the 9 metabolites at 3% (*w*/*w* relative to a total amount of 20 µg/mL) were prepared in the rat plasma extract.

Table 1. Metabolites used for the simulated metabolite sample.

Analyte	Molecular weight (Da)	Description in literature reference[1]
FLP	*7,177.1*	*-*
5'(n-1)	*6,757.8*	*-*
5'(n-2)	*6,364.4*	*-*
5'(n-3)	*5,971.1*	*-*
5'(n-6)	*4,854.1*	*A*
5'(n-7)	*4,508.8*	*B*
5'(n-9)	*3,869.3*	*C*
5'(n-10)	*3,549.0*	*E*
3'(n-11)	*3,229.8*	*G*
3'(n-12)	*2,910.5*	*H*

Chromatography: A Shimadzu LC-20 series HPLC system was used with water containing 15mM N,N-diisopropylethylamine and 35mM hexafluoro-isopropanol as mobile phase A and methanol as mobile phase B. A gradient from 10–40% B in 9 min with a 2 min wash step at 95% B was used at a flow rate of 0.3 mL/min. The column was a Waters ACQUITY PREMIER Oligonucleotide C18 (2.1 × 150 mm, 1.7 µm, 130 Å) kept at 70ºC. The injection volume was set to 10 µL, resulting in a total amount of 200 ng of oligonucleotides on column.

Mass spectrometry: A SCIEX X500B QTOF system was used in negative polarity using an MRM^{HR} method for the 3 most intense charge states of the FLP and each of the spiked-in metabolites (method details available on request). Collision-induced dissociation (CID) was used and collision energies (CE) were selected that ensured the generation of fragment-rich MS/MS spectra. The parameters for the final MRM^{HR} method are summarized in Table 2.

Table 2. MS parameters.

Parameter	MS	MS/MS
Scan mode	*TOF MS*	*MRM^{HR}*
Polarity	*negative*	
Gas 1	*60 psi*	
Gas 2	*60 psi*	
Curtain gas	*30 psi*	
Source temperature	*350°C*	
Ion spray voltage	*-4500 V*	
Declustering potential	*-80 V*	
CAD gas	*7*	
Start mass	*600 m/z*	*150 m/z*
Stop mass	*2,000 m/z*	*3,000 m/z*
Q1 resolution	*N/A*	*Low*
Accumulation time	*0.2 s*	*0.03 s*
Collision energy	*-10 V*	*available upon request*
CE spread	*0 V*	*5 V*
Time bins to sum	*6*	*12*
QJet RF amplitude	*190 V*	*190 V*

Data processing: The molecular weight (MW) of the FLP and metabolites was confirmed by reconstruction using the Bio Tool Kit in the SCIEX OS software. Data were processed using the SCIEX Molecule Profiler software (v.1.2) for identification and relative quantification of the FLP and metabolites. Considering the structure of the oligonucleotide, the number of bonds to break in the parent structure and a comprehensive list of possible transformations (77 for the work presented), the software identifies the different charge states of potential metabolites. This assignment is based on the *m*/*z* match, a 10 ppm tolerance was used for the work presented in this technical note and the match between the measured and

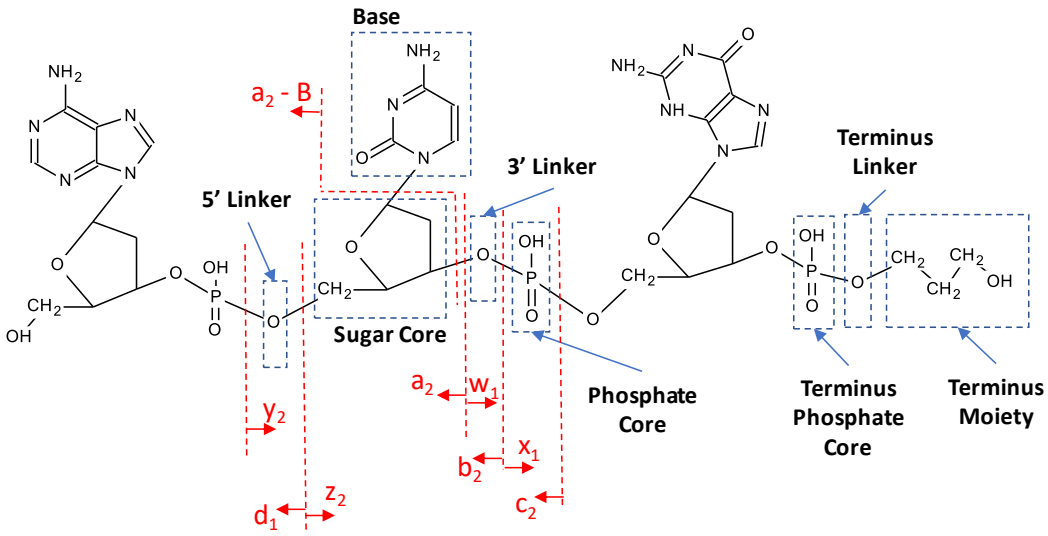

Figure 2. Representation of an oligonucleotide showing the different groups that can be defined for custom nucleotides. Also, the nomenclature of the MS/MS fragments used for sequence confirmation is shown in this figure, taken from the Molecule Profiler software.

theoretical isotope patterns. Additional transformations can be added, while also custom nucleotide residues can be used by defining the 5' and 3' linkers, sugar, base and phosphate groups (Figure 2). The list of found potential metabolites can be manually curated, and the different charge states of each potential impurity are grouped together for relative quantification based on the TOF MS data.

For confirmation of the structure of each potential impurity, MS/MS spectra can be automatically annotated with *a*, *b, c, d, w*, *x* and *y* fragments, including allowing for possible water and base losses (see Figure 2). Sequence coverage is automatically determined by the software, considering user selectable fragment types, signal-to-noise ratio and number of bonds to break. A map of the proposed sequence indicating the fragments that MS/MS evidence was found for is shown, facilitating an easy view of sequence coverage.

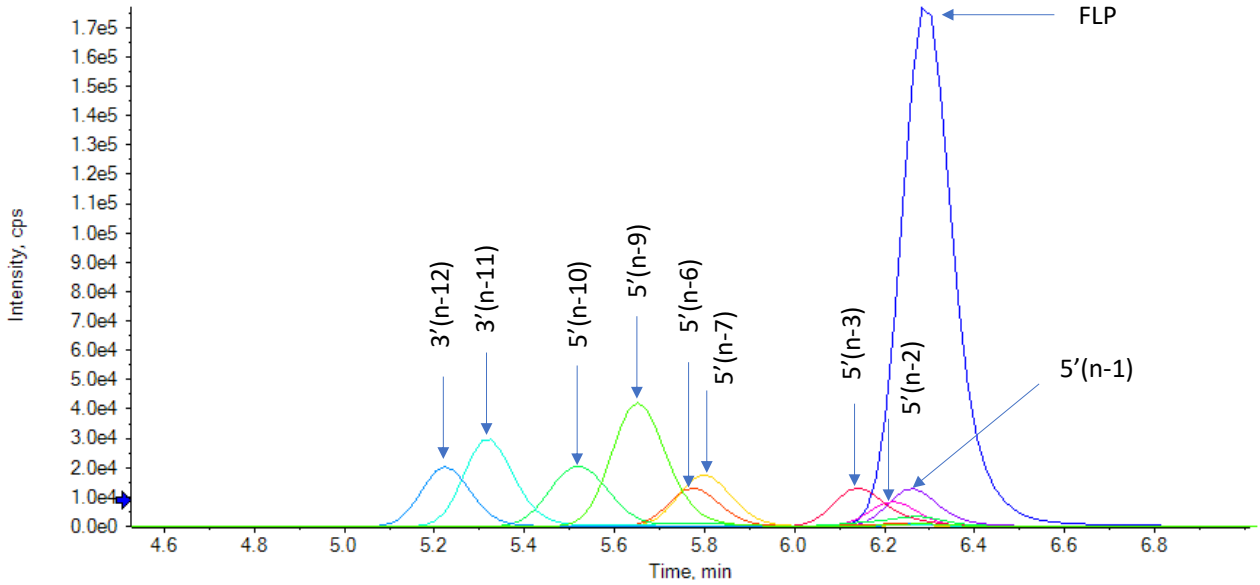

Figure 3. Extracted ion chromatograms (XIC) of the FLP and all spiked-in metabolites. One charge state for each of the analytes from the TOF MS data were used for XIC generation. Good separation from the FLP was achieved for most of the metabolites.

Chromatography

While chromatographic separation between the FLP and metabolites, which are only 1 or 2 nucleotides shorter in length is difficult, most of the metabolites could be separated from the FLP (Figure 3). Separation from the FLP is important, as the multiple charge states from both the FLP and metabolites can result in overlap on the *m/z* axis, interfering with correct identification and relative quantification.

MW determination using SCIEX OS software

As an example, Figure 4 shows the TOF MS spectrum of the C metabolite (5'(*n*-9)) acquired with the X500B QTOF system, a zoom-in of the -6-charge state and the reconstructed mass as calculated by the Bio Tool Kit software add-on that is part of SCIEX OS software. The high-resolution of the X500B QTOF system allows for baseline separation of the isotopes of each charge state. Excellent mass accuracy was observed. For the -5-charge state the mass accuracy of the monoisotopic isotope was -3.8 ppm and that of the reconstructed monoisotopic mass was -1.7 ppm.

Table 3. Mass accuracies for the FLP and all spiked-in metabolites.

Analyte	Theoretical monoisotopic mass (Da)	Mass error (ppm)
FLP	*7,172.09168*	*-3.86*
5'(n-1)	*6,753.02523*	*-3.74*
5'(n-2)	*6,359.94927*	*-3.82*
5'(n-3)	*5,966.87331*	*-2.57*
5'(n-6) (A)	*4,850.70262*	*-3.22*
5'(n-7) (B)	*4,505.67294*	*-1.98*
5'(n-9) (C)	*3,866.61057*	*-1.70*
5'(n-10) (E)	*3,546.58737*	*-1.23*
3'(n-11) (G)	*3,227.54819*	*-0.99*
3'(n-12) (H)	*2,908.50901*	*-0.35*

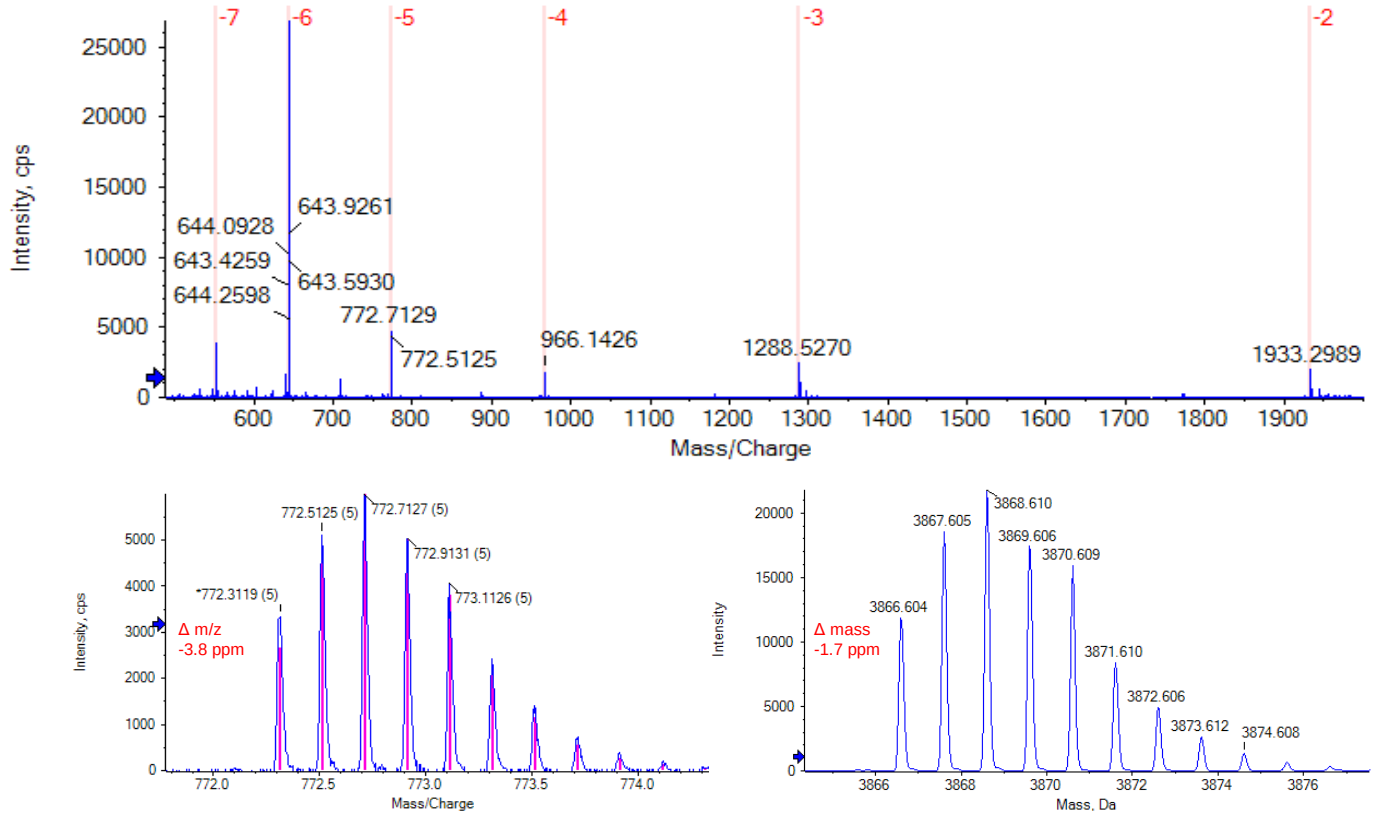

Figure 4. MS spectrum of the 5'(*n*-9) metabolite. Top shows the full spectrum with the charge state envelope from -2 to -7. The bottom shows a zoom-in of the -5-charge state (left) and the isotopically resolved reconstruction with a step mass of 0.03 Da (right). Mass error was -3.8 ppm for the monoisotopic peak of the -5-charge state and -1.7 ppm for the monoisotopic mass in the reconstructed spectrum.

Table 3 summarizes the mass errors of the measured, reconstructed monoisotopic masses for the FLP and the spiked-in metabolites.

Identification and relative quantification of FLP and impurities based on TOF MS data

The Molecule Profiler software was used to identify the FLP and metabolites. Figure 5 shows 2 examples of the match between the measured MS spectrum and the theoretical isotope pattern for the -6-charge state of the 5'(*n*-9) and -5-charge state of the 3'(*n*-11) metabolites. The excellent match between theoretical and measured *m/z* profiles allows for confident identification of these and other metabolites. Figure 6 shows the top 15 of 82 identified potential impurities by %area after grouping charge states for an injection of the ASO-20PS2MOE-FLP spiked with 3% (of total weight) of each metabolites. The scoring was selected to be performed on the isotope ratio matching only, while an *m/z* tolerance of 10 mDa was used for searching. A 40% cut-off percentage for the score was used to ensure only charges states with a good match of the isotope ratio were reported. Charge states from -3 to -11 were considered and only terminal fragments were allowed for the search. When multiple potential metabolites were listed for a specific peak, the lowest scoring metabolite was manually removed. All 9 spiked-in metabolites were found in the top 15 reported potential metabolites. The high % of the desulfurization product was likely caused during sample storage.

Table 4. Average %areas measured for the different 5'(*n*-1) spike-in levels. As the spiked-in shortmer was only 76% pure as determined by TOF MS and Molecule Profiler software, the measured values were in very good correlation with the spiked-in amounts.

Metabolite	Average %area in FLP	Average %area in 3% spike-in	RSD %area in 3% spike-in
5'(n-1)	*0.21*	*3.23*	*9.20*
5'(n-2)	*0.11*	*2.94*	*4.65*
5'(n-3)	*0.41*	*4.00*	*6.34*
5'(n-6) (A)	*0.79*	*3.83*	*5.28*
5'(n-7) (B)	*0.24*	*5.07*	*4.55*
5'(n-9) (C)	*0.42*	*7.73*	*2.79*
5'(n-10) (E)	*1.30*	*6.65*	*6.02*
3'(n-11) (G)	*0.00*	*2.71*	*4.49*
3'(n-12) (H)	*0.00*	*2.60*	*6.17*

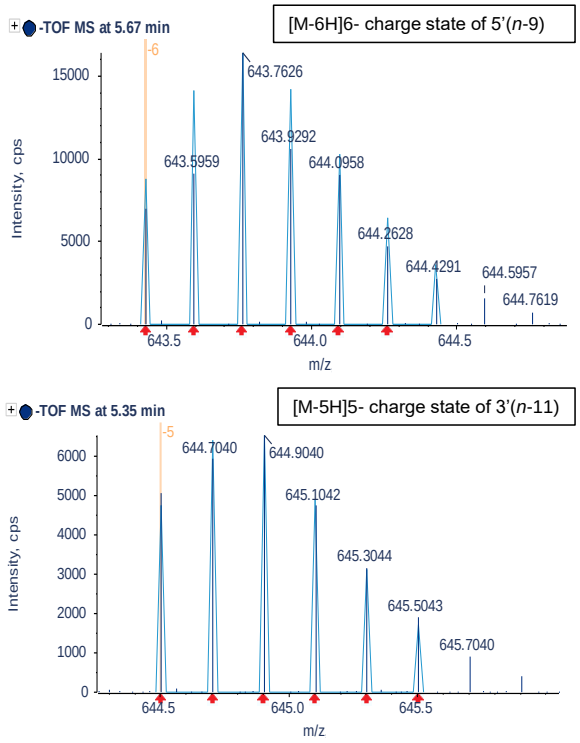

Figure 5. Comparison of the observed *m/z* and theoretical information for 2 metabolites. An excellent match between the theoretical isotope distribution (light blue) and the centroided MS data (dark blue) of the [M-6H]6- charge state of the 5'(*n*-9) metabolite (top) and [M-5H]5- charge state of the 3'(*n*-11) metabolite (bottom) was observed. Dotted yellow line highlights the monoisotopic peak with identified charge state.

82 Groups of 187 Potential Metabolite Peaks

Name	Neutral Mass	ppm	% Area	Count
Parent	7172.05	-5.2	35.35	7
5'(n-9)	3866.59	-4.4	7.81	5
5'(n-10)	3546.57	-4.9	6.67	5
5'(n-7)	4505.65	-4.4	5.17	7
5'(n-6)	4850.68	-5.3	3.94	6
5'(n-3)	5966.84	-5.0	3.89	8
Desulfurization	7156.07	-8.2	3.56	4
5'(n-1)	6752.98	-5.7	3.10	6
5'(n-2)	6359.91	-4.9	3.00	7
3'(n-11)	3227.53	-4.1	2.77	4
3'(n-12)	2908.50	-4.3	2.67	3
3'(n-6)	4851.68	-1.5	2.35	2
Loss of A	7036.99	-8.2	1.54	2
5'(n-10)+Desulfurization	3530.60	-4.6	1.51	5
Phosphorylation + Depyrimidination of U	7158.08	5.6	1.39	2

Figure 6. Top 15 of 82 identified potential impurities. Sorted by %area after grouping charge states for an injection of the ASO-20PS2MOE-FLP spiked with 3% (of total weight) of each of the metabolites. "Count" shows the number of charge states of the impurities that were found. When multiple potential metabolites were listed for a specific peak, the lowest scoring metabolite was removed. All 9 spiked-in metabolites were identified.

Although in-source formation of this product is possible, a difference in retention time for the FLP and desulfurization product was observed, ruling out in-source fragmentation as the cause for the observed desulfurization product.

Table 4 shows a summary of 3 replicate analyses of the spiked-in metabolite sample. Reproducibility of the relative quantification was excellent, with the RSD for each metabolite <10%. The reported relative areas for the metabolites were in-line with the spike-in, except for B, C and E analytes which were reported to be 1.7 to 2.5x higher as the calculated spike-in. Metabolite E was present in a significant amount in the control sample (FLP without spike-in), which can partly explain the higher relative amount reported for this metabolite. In addition, it is possible that (some of) the other analytes used for spike-in contained B, C and/or E analytes, derived from the serial synthesis approach of the ordered analytes.

Confirmation of structures using MS/MS data

For the FLP and spiked-in metabolites MS/MS data were acquired using an MRM^{HR} method. The Molecule Profiler software was used to annotate the peaks in the spectra and to generate a sequence coverage map. Figure 7 shows part of the raw MS/MS spectrum of the -6-charge state of the 5'(*n*-9) metabolite and the corresponding, deisotoped spectrum in the Molecule Profiler software. The doubly charged *y*4 ion was automatically assigned by the Molecule Profiler software. Figure 7 also shows that using MS/MS data derived from the -6 charged precursor only, full sequence coverage with evidence for the position of each nucleotide was achieved. A minimum S/N setting of 50 was used for the assignments and only *a*, *c*, *d*, *w* and *y*-ions were considered with the possible loss of 1 H_2O molecule.

Figure 8 shows a summary of the sequence coverage found based on the MS/MS spectra for the FLP and all spiked-in metabolites. Except for the 5'(*n*-6) metabolite, sequence coverage was 100% for the metabolites. To enable easy review of information, the software combines assigned fragments from the MS/MS spectra from all charged states for a given metabolite. This can improve sequence coverage significantly, as some fragments might only be generated from specific charge states.

Conclusions

- Confident identification of metabolites spiked-in at the 3% (*w*/*w*) in a plasma extract sample was achieved with excellent TOF MS data quality and mass accuracy of the X500B QTOF system
- Relative quantification using Molecule Profiler software showed good correlation of the reported relative amount with the spike-in percentage with excellent reproducibility (RSD <10%)
- The confirmation of the structure of oligonucleotide-based drugs and impurities is greatly accelerated by automatic annotation of TOF MS/MS spectra with the most commonly found fragment ions based on a proposed structures in Molecule Profile software

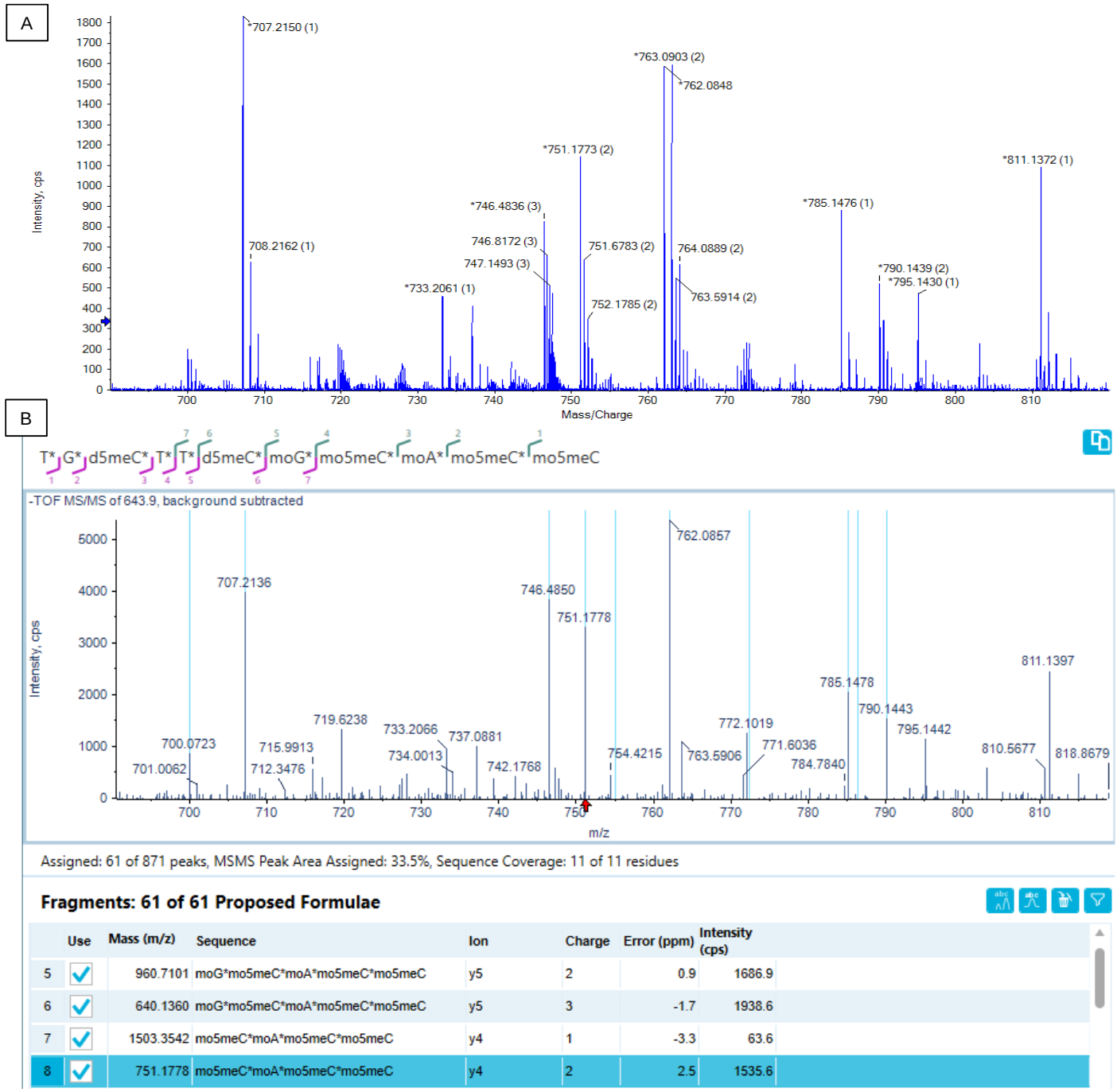

	Use	Mass (m/z)	Sequence	Ion	Charge	Error (ppm)	Intensity (cps)
5	✓	960.7101	moG*mo5meC*moA*mo5meC*mo5meC	y5	2	0.9	1686.9
6	✓	640.1360	moG*mo5meC*moA*mo5meC*mo5meC	y5	3	-1.7	1938.6
7	✓	1503.3542	mo5meC*moA*mo5meC*mo5meC	y4	1	-3.3	63.6
8	✓	751.1778	mo5meC*moA*mo5meC*mo5meC	y4	2	2.5	1535.6

Figure 7. Confirmation of the sequence of the 5'(*n*-9) metabolite using MS/MS of the [M-6H]6- charge state. A zoom-in of the raw MS/MS spectrum is shown on top (A). To enable easier data review, the MS/MS spectrum was de-isotoped in the Molecule Profiler software (B). Using *a*, *c*, *d*, *w* and *y* terminal ions and allowing for 1 water or base loss, the full sequence could be confirmed considering fragments with a minimal S/N ratio of 50.

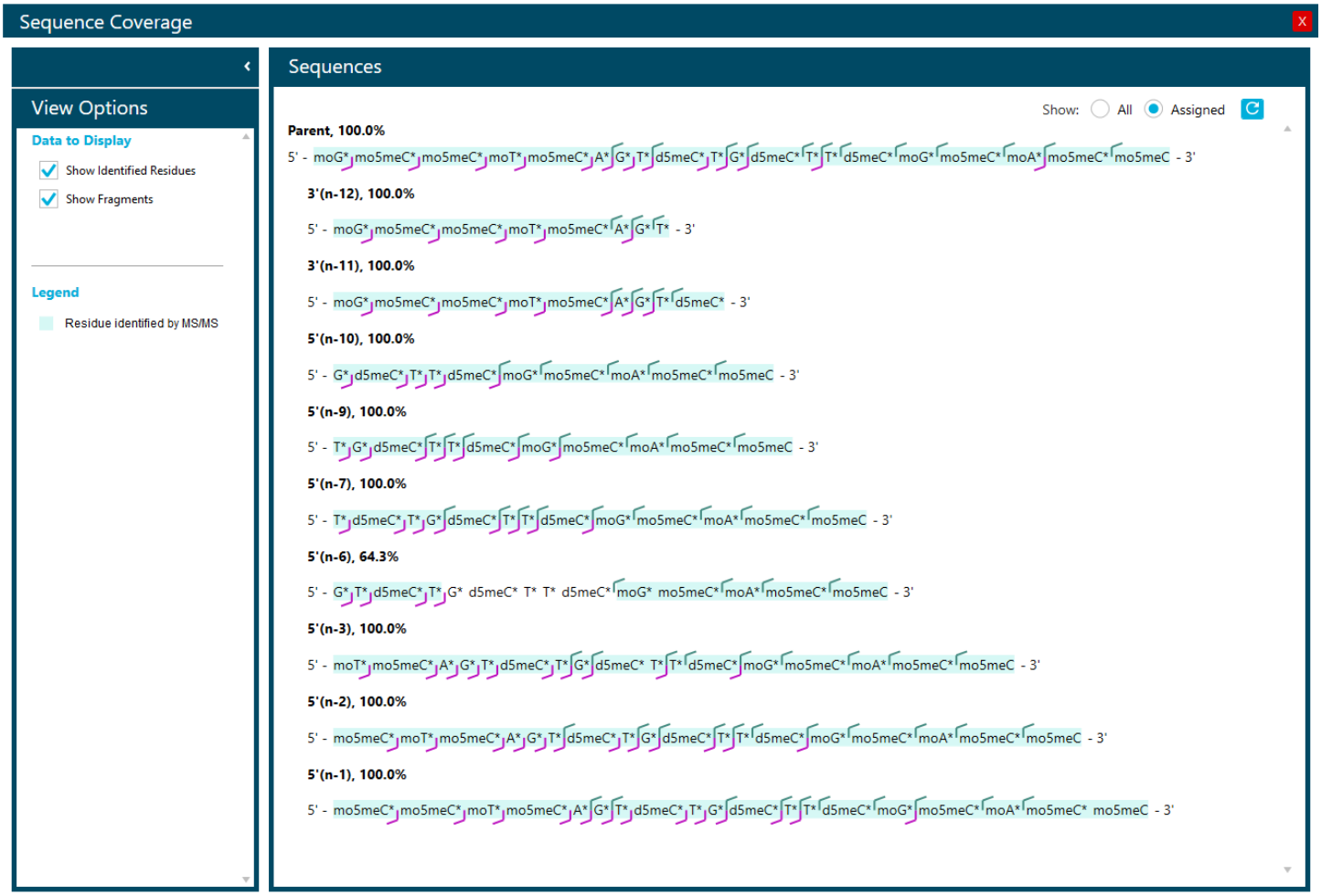

Figure 8. Summary of sequence coverage for the FLP (Parent) and all spiked-in metabolites. Sequence coverage is determined using fragments assigned in all identified charge states of a metabolite that MS/MS spectra were acquired for. *A*, *c*, *d*, *w* and *y* terminal ions were considered and 1 water or base loss was allowed. A minimum S/N ratio of 50 was used.

References

1. Richard S. Geary, Brenda F. Baker, Stanley T. Crooke. Clinical and Preclinical Pharmacokinetics and Pharmacodynamics of Mipomersen (Kynamro®): A Second-Generation Antisense Oligonucleotide Inhibitor of Apolipoprotein B. Clin Pharmacokinet (2015) 54:133–146

Headquarters
500 Old Connecticut Path | Framingham, MA 01701 USA
Phone 508-383-7700
sciex.com

International Sales
For our office locations please call the division headquarters or refer to our website at
sciex.com/offices

Global proteome profiling of CRISPR/Cas9 induced insertions and deletions

Featuring SWATH® Acquisition on a TripleTOF® 6600+ LC-MS/MS System

Michal Lubas[1], Thomas Eriksen[1], Malene Ambjørn[1], Eric Paul Bennett[2,3], Ignacio Ortea[3], Jens-Ole Bock[3], Ferran Sanchez[4], Antonio Serna-Sanz[4], Kerstin Pohl[5]

[1]H. Lundbeck A/S, Denmark; [2]Copenhagen Center for Glycomics, Department of Odontology, Faculty of Health Sciences, University of Copenhagen, Denmark; [3]COBO Technologies, Denmark; [4]SCIEX, Spain; [5]SCIEX, US

Recent advances in gene editing technologies have revolutionized biomedical research. Some technologies enable the introduction of specific single nucleotide changes, insertions and deletion (InDels) in genomes of cells, tissues and whole organisms of any species opening the door for treatment of a variety of genetic-based diseases.[1] In this regard, CRISPR/Cas9 has been widely adopted as the first choice of gene editing modality in the field, due to its simple mode of action and great flexibility in use.[2] With CRISPR/Cas9 moving from a research tool into adaption as personalized medicine, safety concerns have to be addressed: an understanding of the effects on the targeted gene, but also potential off-target effects is desired. Analytical methods such as polymerase chain reaction (PCR)-based methods are widely used. However, the verification on gene level, does not reveal direct information on the protein expression. Immunoblotting techniques can give further insights, but the approaches are limited to the availability of antibodies and furthermore only provide information on the targeted proteins. Mass spectrometry in comparison allows for unbiased information on all detectable proteins addressing the need for understanding the overall impact of gene therapies. Still, challenges such as limited sample amount, sensitivity, specificity and last but not least reproducibility for simultaneous relative quantification on all proteins in a sample need to be overcome. Here, an MS-based strategy is described addressing these additional challenges.

Key features of SWATH Acquisition for CRISPR proteome profiling

- Unbiased MS method without the need for antibody production or extensive method development
- Quantitative analysis with extremely high sensitivity and specificity at the MS/MS level for highly accurate and reproducible results
- Quantification of the target product, but also monitoring of changes in the total proteome, thus exploring the overall impact of gene editing on the protein expression, serving a need to ensure safe therapies

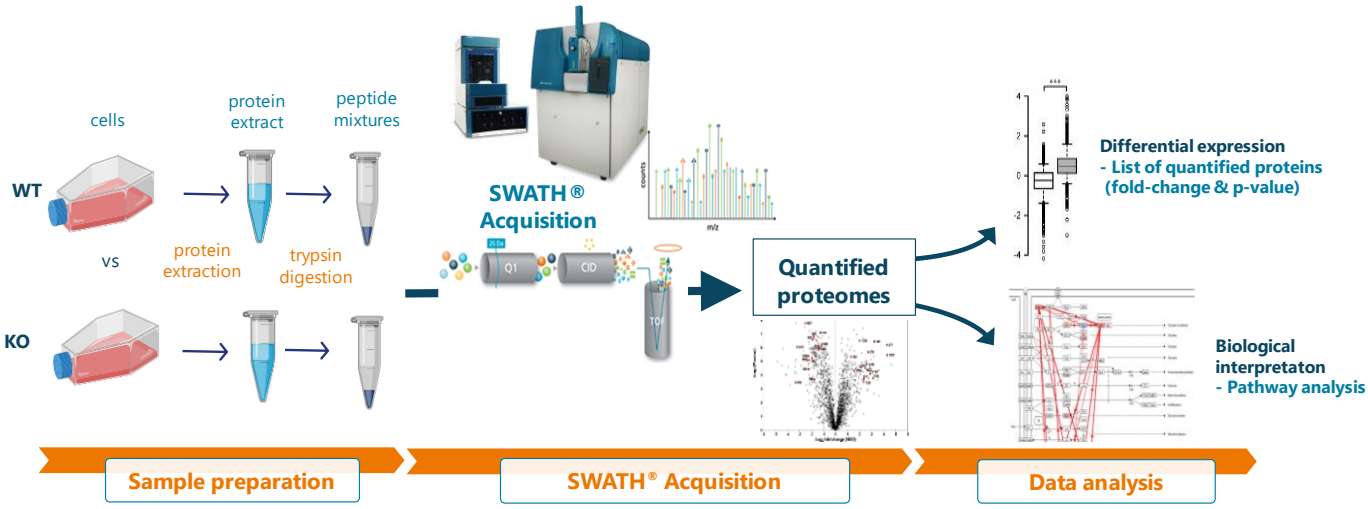

Figure 1: Overview of the proteome expression analysis platform (PIPPR). Proteins of wildtype (WT) and treated cells, e.g. knock-out (KO) cells are extracted and digested followed by LC-MS/MS analysis using SWATH Acquisition. Differential expression are evaluated based on fold-change and p-value, and affected pathways are analyzed to enable biological interpretation of results.

- Functionality-based bioinformatics post-acquisition enables interpretation of large-scale proteomics data providing biologically meaningful results

Methods

CRISPR/Cas9 targeting and validation: The human gene OTUB1 coding for ubiquitin thioesterase OTUB1 was targeted using guiding ribonucleic acid (gRNA) sequences: OTUB1-gRNA1 (5'-CGATAGAAACAGTTGCCGTC-3') or OTUB1-gRNA3 (5'-GACGGCAACTGTTTCTATC-3') (ThermoFisher, TrueGuide). Both gRNAs were functionally validated by IDAA using the CRISPR InDel Profiling Platform (CIPP)[3] based on previously described protocols[4] In brief, 2 µg Cas9 protein (Thermo Fisher Scientific) and 0.5 µg gRNAs were complexed, and electroporated into $1e^5$ HEK293 cells in a 24-well format (for Western blot analysis) or $1e^4$ cells for 96 format (for IDAA analysis). Five days post transfection, cells where harvest by trypsinization and washed with phosphate buffered saline (PBS), spun down at 1000×g, lysed in 50 µL COBO extraction buffer and analyzed by IDAA. InDel detection and profiling by IDAA is based on a PCR using three primers (tri- primer principle): two gene specific primers; in this case specific for OTUB1 A (FAM-seq-5'-TCCTTAAGTGCCCAGCTTCC-3') and B (5'-TGCAACTCCTTGCTGTCATC-3'), that span across the OTUB1 target site, and a third universal fluorescein-labeled primer (FAM-5'-AGCTGACCGGCAGCAAAATTG-3') that is specific for an extension present on one of the gene specific primers (A-primer). Amplicons were size-discriminated by capillary electrophoretic (CE) fragment analysis using a standard DNA-sequencing instrument (Thermo Fisher Scientific). The InDel profiles were generated from the raw data files using ProfileIt-V2 software available from COBO Technologies.[5]

Sample preparation for MS analysis: A HEK293 knock-out cell line and a non-targeted control cell line were used for this study. Samples were prepared as follows: cells were collected in ice-cold PBS and stored as pellets at -80°C. Cell lysis was performed by incubation for 10 min in boiling lysis buffer (6 M guanidine chloride (Gua-HCl), 5 mM tris(2-carboxyethyl)phosphine, 10 mM iodoacetic acid and 100 mM tris(hydroxymethyl)aminomethane (Tris) pH. 8.5) followed by a sonication step. Samples were diluted to 2M Gua-HCl and LysC protein digest performed using 1:200 (*w*:*w*) enzyme:protein ratio for 1 h at room temperature. Samples were further diluted to 0.6M Gua-HCl with 25 mM Tris, pH 8.5 and a second digestion step was carried out overnight with trypsin (1:20 (*w*:*w*)). Protease activity was quenched by acidification with trifluoroacetic acid to a final concentration of approximately 1%, and the resulting peptide mixture was desalted using StageTips (100 µL, Pierce).

Chromatography: 2 µg of the tryptic digested sample were separated by reversed-phase chromatography using a SCIEX NanoLC™ 425 HPLC System in low microflow configuration (5 µL/min) equipped with a YMC Triart column (150×0.3mm, particle size 3 µm, pore size 12 nm). Mobile phase A consisted of water with 0.1% formic acid, while mobile phase B consisted of acetonitrile with 0.1% formic acid. A gradient from 8% to 30% mobile phase B within 30 min and 40°C column oven temperature was applied. The column was washed during 5 min at 95% B and equilibrated during another extra 5 min at 5% B before the next injection. Same separation and injection conditions were used for library generation via information-dependent acquisition (IDA) runs as well as data-independent acquisition (SWATH Acquisition).

Mass spectrometry: For library generation and sample testing, data were acquired in replicates on the TripleTOF 6600+ System using an IDA method monitoring the 100 most intense peaks within a total cycle time of 2.5 s. SWATH Acquisition data were acquired using a method with 100 variable windows and 25 ms accumulation time for each window.

MS data processing: For ion library generation, a combined search of six IDA replicates per sample was done using ProteinPilot™ Software 5.0, resulting in 3556 protein groups with an FDR cut off of 1%. SWATH Acquisition data were subsequently processed using OneOmics™ Project in SCIEX Cloud and on a local workstation using the SWATH Acquisition MicroApp 2.0 within PeakView® Software 2.2 and MarkerView™ Software 1.3 deploying the previously generated ion library.

Analytical tools for CRISPR/Cas9

All current gene editing technologies share the common principle of inducing a DNA double strand break (DSB) at a user-specified site in the genome, followed by cellular repair of the induced DSB. In mammalian cells, the non-homologous end joining repair pathway dominates the cellular repair and, as a consequence, the primary outcome after gene editing is the formation of InDels at the targeted site. When the target site is chosen to be positioned in the protein encoded gene sequence (exon), these gene editing induced InDels can result in disruption of the protein encoded reading frame (out-of- frame causing InDels), which leads to abrogation of gene function. In these so-called knock-out (KO) gene editing experiments, the primary objective is to induce a high frequency of these out-of-frame causing InDels, that can be detected by genetic analysis of cells after gene editing.

Among the available InDel detection methodologies, InDel Detection by Amplicon Analysis (IDAA) has shown great promise as a fast, robust and cost efficient method, with InDel detection

sensitivity being comparable to next generation sequencing.[6,7] However, InDel detection and profiling will only provide genetic information of the induced gene editing events at a specific genomic site. When working with cell populations, tissues or whole organisms, it does not reveal what consequences it might inflict at the protein level for the gene of interest, or globally at the proteome level.

Alternatively, immunoblotting assays can be applied for this purpose, but the use of antibodies has several drawbacks: in many cases there are no antibodies available for the target protein. Even in the cases where antibodies are available, they are limited to given epitopes and can suffer from low specificity because of cross-reactivity, poor quality or batch-to-batch variability. As a consequence of gene editing, non-desired, off-target changes can occur, which are difficult to be detected and measured reliably, as they can be located throughout the genome. Since they are not known at the outset, targeted methods such as specific antibodies cannot be used to detect such changes.

In comparison, mass spectrometry (MS)-based techniques offer high resolution and specificity, thus, it can be used to confirm that the gene editing resulted in the desired effect at the protein level in an unbiased way. In addition to measuring the expression of protein product of the edited gene, MS experiments can provide information on the global proteome expression. This allows for detection of off-target editing events and mapping of differentially regulated proteins in one effort. However, a few challenges need to be overcome. In order to provide a full picture of the changes in a given heterogenous sample, all analytes need to be detected with high sensitivity, specificity and reproducibility. Furthermore, quantitative information on all of the analytes—from high abundance to very low abundance—in a complex matrix is desired.

Verification of CRISPR/Cas9 target by PCR using CIPP

OTUB1 has recently been reported to impact the clearance of aggregated Tau protein.[8] Thus, there is interest to better describe the function and cellular processes in which OTUB1 may play a role in connection with Alzheimer's disease pathology.

The target validation of OTUB1 by CRISPR/Cas9 was performed using IDAA. IDAA is based on a PCR with a tri-primer principle: two OTUB1 gene specific primers A and B that span across the OTUB1 target site, and a third universal, labeled primer that is specific for an extension present on one of the gene specific primers (A-primer). The tri-primer methodology ensures homogeneous labeling of amplicons that are subsequently size-discriminated and detected by CE analysis. For the cells targeted with gRNA1, gRNA3, the wild type (WT) and the non-transfected (NT) cells, the amplification of the target gene OTUB was proven to be successful using the tri-primer principle (Figure 2B). The subsequent CE analysis revealed InDels of various lengths in the gRNA1 and gRNA3 targeted cells (Figure 2C), while the amount of the expected length of the OTUB gene product (yellow peak in Figure 2C) was significantly decreased compared to the WT and NT cells. Since a cell population can contain a mixture of cells which were successfully treated with the CRISPR/Cas9 approach and such cells which weren't, there can be still evidence of the gene of interest (yellow peak in Figure 2C for gRNA1 and gRNA3). The WT and NT cells did not show any additional peaks, as expected. Overall, these results prove the successful CRISPR/Cas9 targeting on gene level.

InDels leading to disruption of the protein encoded reading frame (out-of-frame InDels) were indicated in blue (Figure 2C) and the total percentage compared to the wildtype was calculated (Table 1). InDels which didn't lead to a disruption of the reading frame were indicated in white (Figure 2C). The sum of both types of InDels was used for the quantification of total InDels for both targets (gRNA1 and gRNA3, Table 1): The gene inactivation efficiency in the cell pool of 5×10^6 cells was determined by CIPP with overall InDel formation efficiencies of >91% and importantly, with out-of-frame causing InDel efficiencies >80% (Table 1). Out-of-frame InDels are desired as they usually lead to the abrogation of gene function, whereas in-frame InDels might not.

Table 1: OTUB1 gene editing induced InDel profiles for samples targeted with gRNA1 and gRNA3. Percentages calculated based on peak area of CE analysis**.**

Sample	Total InDels* [%]	Out-of-frame InDels* [%]	InDels in size (percentage)^
gRNA1	*91.0*	*80.1*	*1 (50.4%) -1 (8.6%) -8 (6.0%) -6 (5.6%) -10 (3.9%) -7 (2.1%) -9 (1.8%) -2 (1.5%) -3 (1.5%) -4 (1.4%)*
gRNA3	*94.8*	*85.8*	*1 (58.5%) -4 (6.9%) -12 (4.5%) -8 (3.7%) -16 (3.4%) -2 (3.2%) -10 (1.9%) -5 (1.8%) -9 (1.7%) -1 (1.4%)*

*calculated including wildtype and unmodified alleles
^10 most abundant InDels with % detected peak area indicated in parenthesis

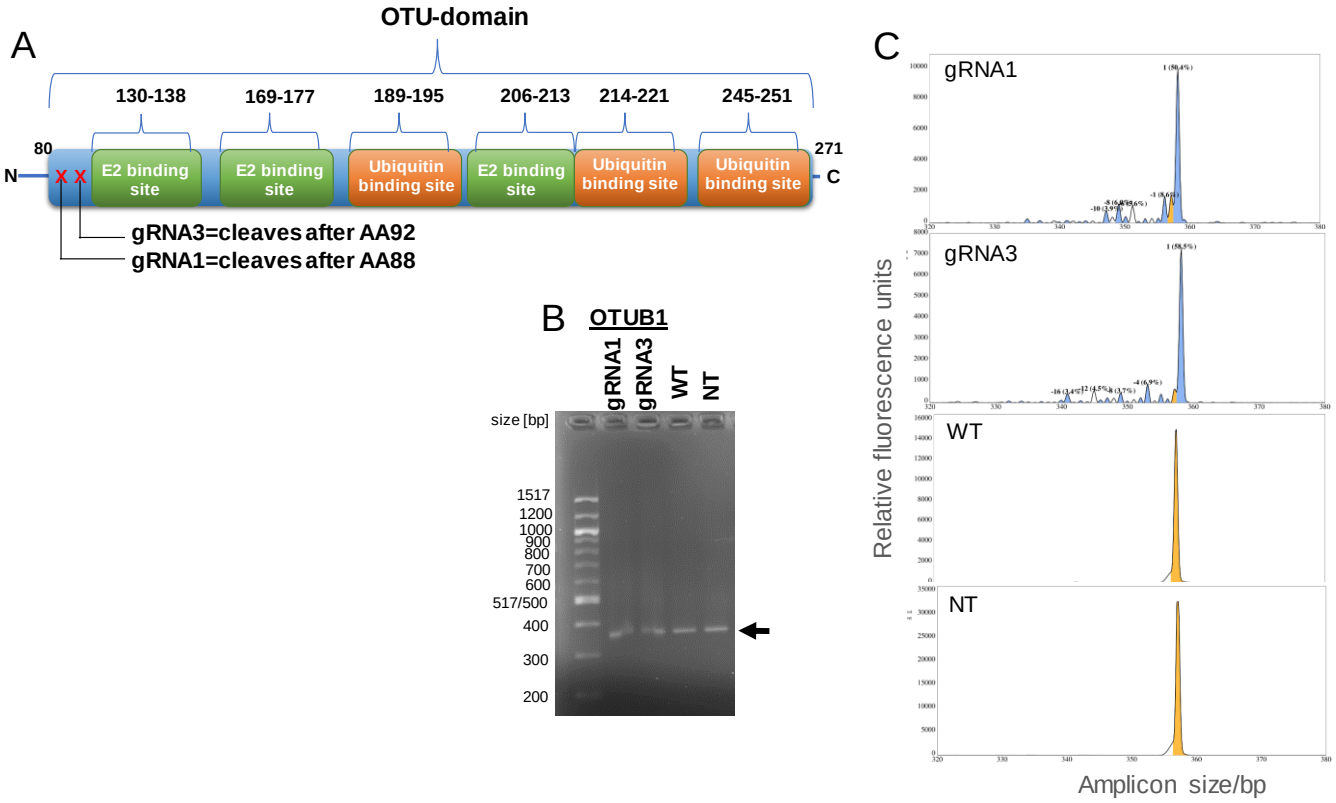

Figure 2. CIPP analysis after CRISPR/Cas9 OTUB1 gene targeting of gRNA1 and gRNA3 in human HEK293 cells. A: Illustration of OTU domain structure with indication of the regions targeted (gRNA1 and 3, indicated with red crosses). B: Gel electrophoresis results of tri-primer amplification of OTUB1 target locus after Cas9/OTUB1-gRNA1 or -3 editing showing a single specific fluorophore-labelled amplicon in HEK293 edited samples (indicated by arrow); gRNA1, gRNA2, wild type (WT) and non-transfected (NT) cells. C: CIPP functional validation and profiling of gRNA1 and -3 InDel formation potential, showing >90% efficiency and no InDel formation in WT nor NT cells. Peak profiles were generated by IDAA fragment analysis and ProfileIt-V2 profiling displaying unmodified alleles in yellow, out-of-frame InDel possessing alleles in blue and in-frame InDel alleles in white. Insertions and deletions are displayed to the right and left of the unmodified yellow peak, respectively. Top five observed InDels are indicated above peaks and calculated total frequencies shown in Table 1.

Evaluation of expressional changes

CRISPR technology was used to create an OTUB1 gene KO HEK293 cell line and SWATH Acquisition was applied to assess the impact of gene-inactivation on the overall changes in the cellular proteome in a quantitative manner.
The high CRISPR/Cas9 OTUB1 knock-out efficiency determined by CIPP was confirmed at the protein level by western blotting and MS (Figure 3 and 4): both protein detection techniques were able to detect OTUB1 protein in unmodified cells and confirmed its knock-out in CRISPR/Cas9-modified cells, which demonstrates the applicability of SWATH Acquisition is an alternative protein detection methodology.

In particular, in experimental settings where antibodies specific towards the protein of interest are not available, alternative methodologies are needed. Additionally, MS analysis is unbiased and provides access to the entire proteome, unlike antibodies targeting specific epitopes. Still, the quantification of analytes via MS poses challenges especially in complex matrices such as cells or tissues since the MS information can suffer from interferences leading to wrong results. Hence, quantification on MS/MS level is favorable as it provides additional specificity. However, for understanding the overall impact of CRISPR/Cas9 technology on the proteome, the target analytes cannot be predefined which limits the usage of standard quantification methods such as multiple reaction monitoring (MRM). Since the data independent approach of SWATH Acquisition provides MS and MS/MS data of the entire mass range in each cycle in a manner compatible with any LC time scale, fragment information can be used for quantification of any detectable analyte without the need to define the target analyte upfront. The spectral, quantification-ready information is stored as a digital fingerprint and proteins of interest for quantification can be defined after acquisition.

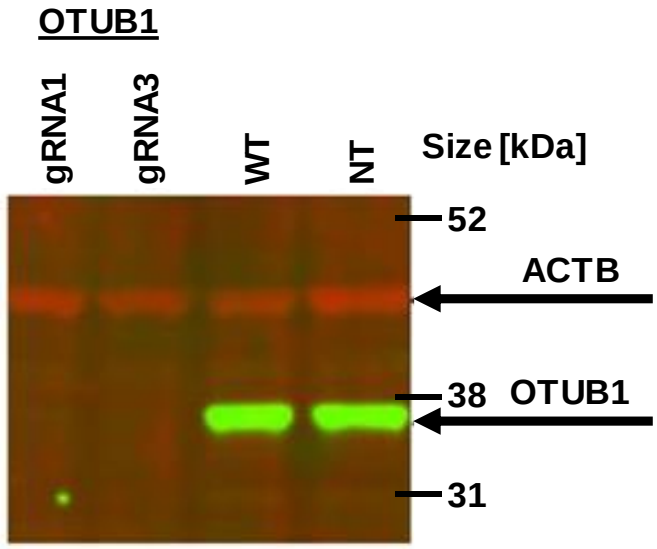

Figure 3: Western blot analysis. Actin (ACTB) serves as positive control, being present in the gRNA1 and gRNA3 targeted cells, the wild type (WT) and the non-transfected (NT) cells. The OTUB1 protein was only detected in the WT and NT cells, indicating a successful knockout in the gRNA1 and gRNA targeted cells.

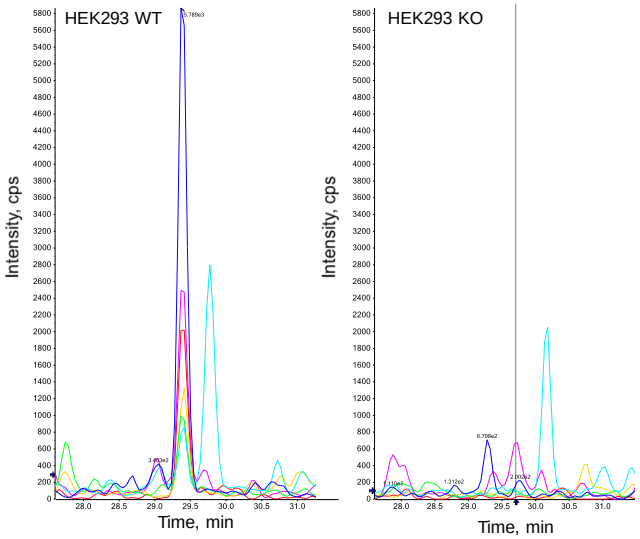

Figure 4: Extracted ion chromatograms (XIC) for fragments of peptide derived from the OTUB1 protein. Example showing the XICs of fragments of a peptide (AFGFSHLEALLDDSK) in the wildtype HEK293 cells (WT) and the knockout HEK293 cells (KO). The KO cell line does not show clear evidence of the specific fragments, indicating a successful knockout compared to the WT.

The data-independent SWATH Acquisition was performed in triplicate resulting in 16550 identified peptides with a CV value of 20% (cut-off applied for quantification, Figure 5). A total of 2819 different protein groups could be quantified based on these peptides (Figure 5).

Principal component analysis (PCA) in MarkerView™ Software based on all MS signals of replicates of control and the OTUB1 targeted KO cells revealed that first two components explained 85% of the total variance (Figure 6). An excellent separation of

A

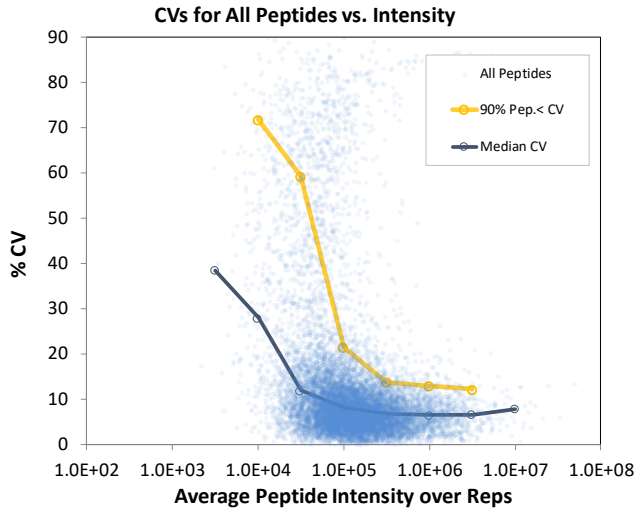

B

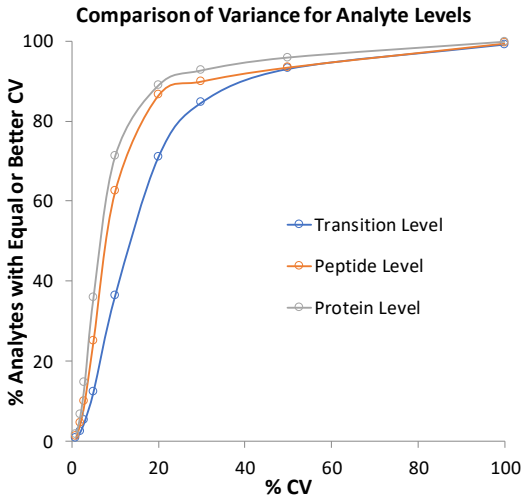

Figure 5: Results of SWATH Acquisition. A: %CV dependence on peptide intensity (n = 3). Peptides below yellow curve with a %CV of 20% or less represent 90% of all peptides. These peptides will be taken into account for quantification. B: Percentage of analytes versus their %CV for fragment (transition) level, peptide and protein level (n = 3). More than 88% of all detected proteins showed a %CV lower or equal to 20% and were used for quantification.

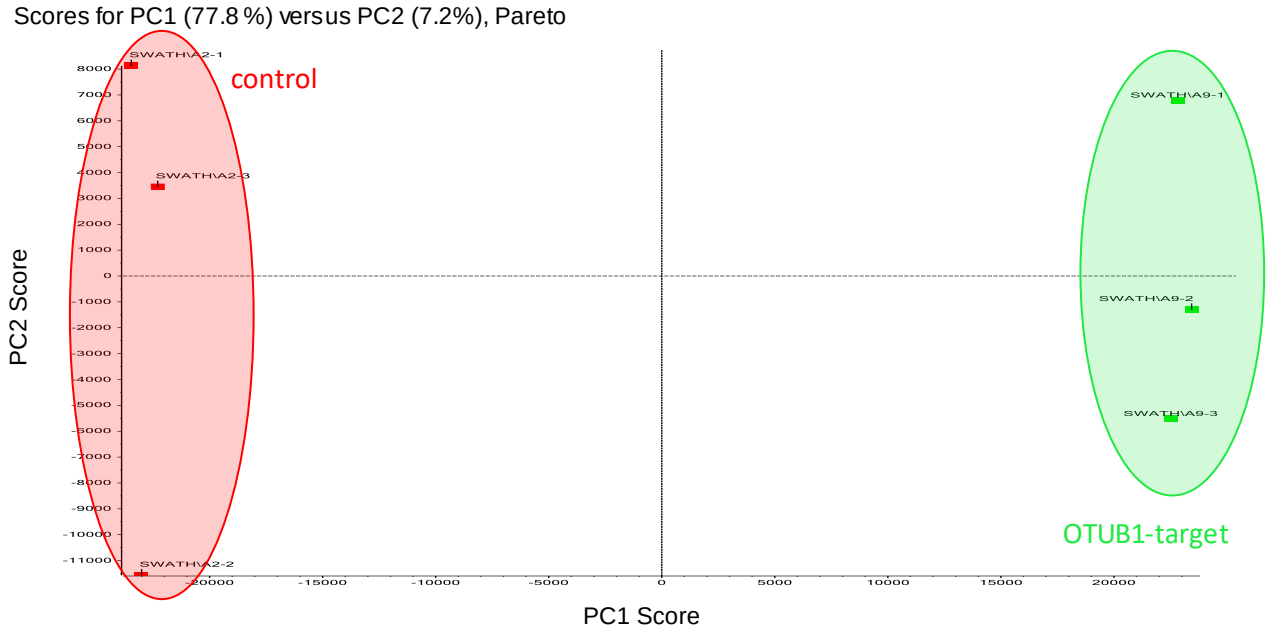

Figure 6: Principle component analysis in MarkerView Software. Scores plot showing 85% of the total data variance (77.8% for PC1 and 7.2% for PC2). Separation based on PC1 was observed for the control and OTUB1 targeted KO cells.

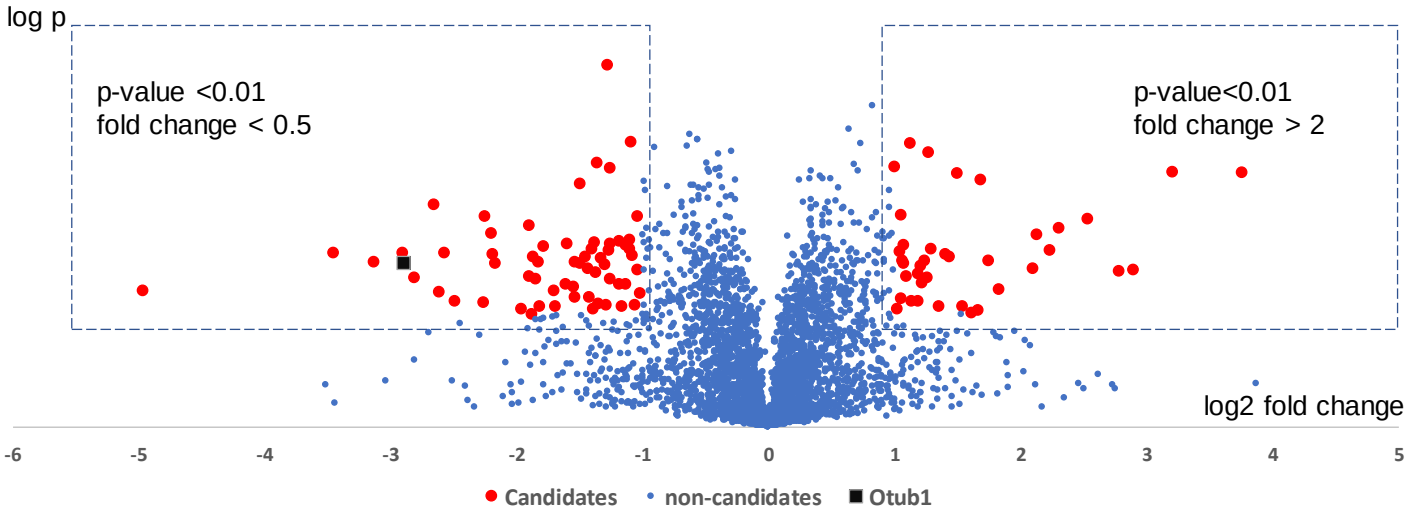

Figure 7: Impact of CRISPR OTUB1-knock-out on proteome level. Volcano plot: representation of binary logarithm of fold changes against decimal log of p-values. Candidates (red) were selected based on lower than 0.5 or higher than 2 fold change (log2<-1 or log2>1) with p values better than 0.01. A total of 100 candidates passed this selection filter. Otub1 protein indicated as black square showing a down-regulation.

the control and the KO cells for the first component was observed (Figure 6).

In total, 100 proteins showed changes when being compared to controls: 62 were down-regulated and 38 up-regulated (Figure 7) when applying the following criteria: a fold change lower than 0.5 or higher than 2 and a p-value lower or equal than 0.01. The subsequent pathway analysis of the deregulated proteins, using the Pathway Browser Reactome (access via OneOmics Project), revealed that affected pathways were mainly related to gene expression, cell cycle progression and DNA repair (Figure 8). This information can be used for in depth analysis of each pathway increasing the understanding of OTUB1's cellular functions.

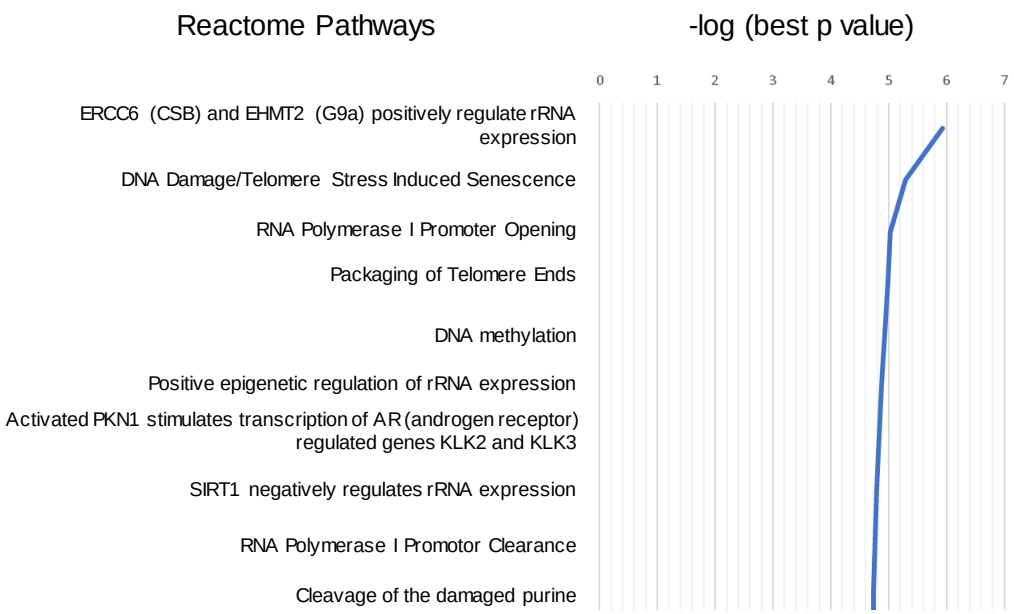

Figure 8: Impact of CRISPR OTUB1-knock-out on Reactome pathways. Ten most affected pathways based on candidate selection as indicated in the Pathway Browser Reactome. Data was filtered using a p-value equal or better than 0.001.

Conclusion

- The successful knockout of the OTUB1 gene in HEK293 cells was confirmed by SWATH Acquisition, in alignment with other protein detection techniques (Western blotting) and genomic-based techniques (PCR-based IDAA)
- The accurate, rapid and robust method presented is not limited to measuring protein expression of a target gene, but can also detect non-desired, off-target events, which may occur across the entire genome, within the same single method
- The functionality-based post-analysis of protein expression data can identify changes in the signal transduction and metabolic pathways allowing for identification of responses at the functional/molecular mechanisms level derived from gene editing
- CRISPR/Cas 9 and SWATH Acquisition are excellent partners.[9] They allow monitoring of the target protein in parallel with thousands of other proteins across sample sets, ensuring reproducibility and accuracy by increasing specificity via MS/MS-based quantification.

References

1. Chandrasegaran S and Carroll D (2016) Origins of programmable nucleases for genome engineering. J. Mol. Biol., **428**, 963–989.
2. Knott GJ, Doudna, JA (2018) CRISPR-Cas guides the future of genetic engineering. Science, **31(6405)**, 866-869.
3. CRISPR InDel Profiling Platform (CIPP) powered by IDAA: https://cobotechnologies.com/services/Indel-profiling/
4. Lonowski LA *et al.* (2017) Genome editing using FACS enrichment of nuclease-expressing cells and indel detection by amplicon analysis. Nat Protoc **12(3)**, 581-603.
5. ProfileIt-V2 software available from COBO Technologies: https://cobotechnologies.com/software/InDel-analysis-software/.
6. Yang Z *et al.* (2015) Fast and sensitive detection of indels induced by precise gene targeting. Nucleic Acids Res **43(9)**, e59.
7. König S *et al.* (2019) Fast and quantitative identification of e vivo precise genome targeting-induced indel events by IDAA. Methods Mol Biol **1961**, 45-66.
8. Wang P *et al.* (2017) Tau interactome mapping based identification of Otub1 as Tau deubiquitinase involved in accumulation of pathological Tau forms in vitro and in vivo. Acta Neuropathol **133(5)**, 731-749.
9. Confirming gene mutation by CRISPR-Cas9 at the protein level and identifying proteome-wide changes. SCIEX technical note RUO-MKT-02-9247-A.

Legal notice

A patent application covering the IDAA method is pending.

CIPP and ProfileIt-V2 are trademarks of COBO Technologies.

Headquarters
500 Old Connecticut Path | Framingham, MA 01701 USA
Phone 508-383-7700
sciex.com

International Sales
For our office locations please call the division headquarters or refer to our website at
sciex.com/offices

SCIEX

The Power of Precision

台灣塞爾克斯應用生技有限公司 | 11492 台北市內湖區瑞光路631號4F
SCIEXNow Toll Free : 0800-818-978 或 service.taiwan@sciex.com